Mesoscale extreme rainfall events in West Africa: The cases of Niamey (Niger) and the Upper Ouémé Valley (Benin)

Eric-Pascal Zahiri, Ibrahim Bamba, Adjoua Moïse Famien, Augustin Kadjo Koffi, Abé Delfin Ochou

Weather and Climate Extremes 13 (2016) 15–34

Contents lists available at ScienceDirect

Weather and Climate Extremes

journal homepage: www.elsevier.com/locate/wace

Mesoscale extreme rainfall events in West Africa: The cases of Niamey (Niger) and the Upper Ouémé Valley (Benin)

Eric-Pascal Zahiri [a,c,*], Ibrahim Bamba [a], Adjoua Moise Famien [a,b], Augustin Kadjo Koffi [a], Abé Delfin Ochou [a]

[a] Laboratoire de Physique de l'Atmosphère et de Mécanique des Fluides, Cote d'Ivoire
[b] Laboratoire d'Océanographie et du Climat, Expérimentation et Analyses Numériques, Paris, France
[c] Recursos Hídricos e Altimetria eSpacial da Amazônia, Universidade do Estado do Amazonas, Manaus, AM, Brazil

ARTICLE INFO

Article history:
Received 23 August 2015
Received in revised form
9 May 2016
Accepted 11 May 2016
Available online 17 May 2016

Keywords:
Extreme rainfall events
West Africa
Return period
IDF curves
Duration
Storm classification

ABSTRACT

In West Africa, a sharp decrease in rainfall has occurred in conjunction with an increase in flood damage since 1970. The material damage and loss of life resulting from floods highlights the undeniable vulnerability of populations to this threat and illustrates the importance of addressing the evolution of hazardous precipitation caused by intense rainstorms. This work aims to improve our knowledge of the behaviour of extreme rainfall in West Africa by studying the sub-hourly, hourly and daily evolution of the most extreme rainfall events, a topic that is especially important to those interested in studying the links between heavy rainfall and flash flooding or inundation. This study analyses the classes of extreme rainfall events in two distinct climatic areas within West Africa using the meteorological scales relevant to rainfall processes. The study is based on two precipitation datasets recorded by dense networks of rain gauges set up within the meso-sites of Niamey (Niger, Sahelian area) and the Upper Ouémé Valley (Northern Benin, Soudanian zone) from 2000 to 2010 and 1998 to 2010, respectively. The Gumbel distribution was used to analyse the frequency of the maximum rainfall series for durations varying from 5 min to 24 h. The reliability of this model was examined, and the Intensity-Density-Frequency (IDF) curves derived from it were used to estimate the critical rainfall intensities at each site. The results returned exceeded frequencies that were useful for the isolation and classification of extreme rainfall cases using temporal characteristics. The climatological results confirm the existence of a latitudinal gradient in the mean annual rainfall and number of extreme events at the mesoscale. The classification methods illustrate clear distinctions between local, meso and synoptic scale events derived from convective systems over the Sahel. In contrast, Soudanian climate conditions lead to a nesting of the phenomena involved in the formation of cloud systems, making it difficult to classify rain events in that area. However, we were able to utilize the duration of rainfall events within this zone to discriminate between types of convective systems that cause extreme rainfall. For both areas, the proportion of precipitation in an extreme event compared to total yearly precipitation served as a suitable additional criterion used to objectively identify extreme precipitation event types.

1. Introduction

In the context of natural climate variations and their cycles, researchers have noticed an increase in floods and inundations in many West African countries in recent years (Panthou et al., 2014). In 2009, twelve member states of the West African sub-region suffered severe inundations (source: Office for Coordination of Humanitarian Affairs (OCHA), October 2009); and between 2000 and 2008, a total of 89 inundation cases were recorded (source: Office of Foreign Disaster Assistance-Centre of Research on the Epidemiology of Disaster (OFDA-CRED)/University of Louvain, Belgium). Tragically, inundations are often repetitive and result in significant, dramatic socio-economic impacts to the areas affected. Increased inundations in recent years demonstrate the high vulnerability of certain populations (Di-Baldassarre et al., 2010); and evidence supports efforts to consider this hazard in adaptation plans, particularly in West Africa, to preserve the region's fragile socio-economic equilibrium.

The underlying causes of such inundations are diverse,

* Correspondence to: RHASA (Escola Superior de Tecnologia-EST), Universidade do Estado do Amazonas, 670 Av. Darcy Vargas, 1200, Parque 10, Manaus, AM CEP 69050-020, Brazil.
E-mail addresses: zahiripascal@gmail.com (E.-P. Zahiri), ibrahimbambino@yahoo.fr (I. Bamba), famienmoise@yahoo.fr (A.M. Famien), kadjoaugustinfr@yahoo.fr (A.K. Koffi), ochou.delfin@gmail.com (A.D. Ochou).

http://dx.doi.org/10.1016/j.wace.2016.05.001

complex, and involve not only the absence of efficient rainwater drainage systems, uncontrolled urban expansion, and the construction in water outlets but also the occurrence of extreme rainfall events or extreme rainfall intensities. Easterling et al. (2000) performed a literature review that highlights an increase in heavy precipitation for two thirds (2/3) of the regions discussed (see their Table 2 and Fig. 2). In addition, numerous recent studies based on both observations and simulations have confirmed these conclusions at the global, regional, and local scales (Alexander et al., 2006; Guhathakurta et al., 2011; Keggenhoff et al., 2014; Min et al., 2011). For example, Keggenhoff et al. (2014) noted an increase in maximum 1-day and 5-day precipitation events, as well as the number of very heavy precipitation days in Georgia at the local scale.

We might reasonably be asked whether the apparent increase in floods or inundations is due to increases in maximum rainfall amounts or significant recurrences of extreme precipitation events. Zhang et al. (2011) reviewed a long series (1960–2002) of daily precipitation data collected across 150 rain gauges and illustrated that the high probability of flood occurrences is related to the increasing trend in extreme rainfall events in the Yangtze River basin (China) region. Thus, an analysis of heavy rainfall events based on estimates of those events' return periods (or return frequency) or changes can suitably be used to investigate and understand the links between those events and floods. Moreover, according to several authors (Pall et al., 2006; Giorgi et al., 2011), the high natural variability of precipitation and the proven impact of climatic warming on the tails of rainfall distributions suggest that researchers will be more readily able to identify climate changes by studying the extreme elements within the hydrological cycle.

Thus, the study of extreme rainfall values is of particular interest to researchers looking at the risks associated with or attempting to identify indicators of climate change. For example, estimates of the recurrence intervals of extreme rainfall events in developing countries, which are determined through the evaluation of the return period of past events, provide data indispensable to the construction and sizing of infrastructure such as storm sewers, drainage systems, bridges and roads in such a way that these facilities effectively protect local populations and prevent hydrologically induced economic disasters. Within hydrological and environmental applications, extreme daily rainfall values can be used to predict potential flooding along rivers; in particular, this information is useful in planning future adaptation strategies such as storm water drainage system designs and flood protection infrastructure in urban areas. Within agro-meteorology, efforts are underway to understand and predict when and where heavy rainfall may damage crops and how this may affect food insecurity (Yabi and Afouda, 2012). In other words, extreme rainfall studies aim to document and assess climate risks in relation to the various sectors affected by the efficient management of hydro-meteorological risk. Such studies can assist planners in the provision of adequate protection and adaptation solutions whose implementation will contribute to the resilience of populations and a reduction in the rate of dramatic socioeconomic disasters.

Surprisingly, research into extreme rainfall events in West Africa is scarce. Most of the work in this region has focused on the analysis of "dry extremes;" and it has been difficult to acquire continuous daily, hourly or sub-hourly rainfall data for periods long enough to identify extreme rainfall events. Nevertheless, New et al. (2006) analysed daily data from six stations in West Africa (two in the Gambia and four in Nigeria) and revealed a rising trend in annual maximum daily rainfall at only one observation site. In Cote d'Ivoire, Goula et al. (2012) analysed annual maximum daily rainfall time series from 34 stations for the period 1947–1995. Using three indices (annual maximum rainfall, number of days where precipitation exceeded a 50 mm threshold, and total days exceeding 50 mm per year), the study highlighted a downward trend in extreme rainfall events. Easterling et al. (2000) addressed heavy precipitation events in various countries around the world and noted that the Sahel region of Nigeria experienced a decrease in maximum daily rainfall rates up to 1997. More recently, Panthou et al. (2014) have investigated changes in extreme rainfall and rainfall regimes in the central Sahel region during the period 1950–2010. Their analysis of select indices over an extended time period allowed them to show that the great drought from 1970 to 1990 was associated with a sharp decrease in extreme rainfall events, including apparent decreases in the intensity of annual maximum daily rainfall values (see their Fig. 3). Their study also noted that the last ten years of the study period were marked by annual cumulative rainfall values generally close to the study's average; however, extreme rainfall events where the values exceeded those observed during the wet period from 1950 to 1969 were increasing.

In Centrafrique, on the edge of this West African zone, Ndjendole and Perard (2003) relied on daily rainfall data collected by 36 rainfall stations from 1951 to 1990 to estimate the return durations of heavy rainfall. They showed that extreme rainfall events with different return periods have different characteristics. For a return period less than 10 years, daily rainfall values of 100 mm are infrequent. However, these types of extreme events become more frequent for return periods equal to or greater than 10 years. In addition, by examining the spatial distributions and origins of these heavy rainfall events, the study showed that extreme rainfall events originate in various ways, including via stormy clouds, squall lines and monsoons. Furthermore, the study indicated that daily extreme values less than 90 mm have no zonal or meridional organization but rather are generally influenced by the local conditions at each station. Indeed, Ndjendole and Perard (2003) indicate that the highest extreme values were concentrated in an area in the centre of the country, where the presence of a river and the Congolese forest favour convection. Conversely, rainfall events associated with a monsoon regime registered by most of the rainfall stations in the south exhibited relatively low extremes.

However, all of the above studies, including the relatively recent works from Panthou et al. (2012, 2014) have focused on the characterization of extreme daily rainfall events in West Africa, which while valuable, fail to address the links between extreme rainfall and flash flooding. Little work on this topic has been done at sub-daily timescales. This is largely because daily measurements readily available from the gauge stations have not allowed researchers to derive statistical characteristics for hourly and sub-hourly periods. The introduction of such hourly or sub-hourly sampling durations could facilitate more detailed analyses, particularly since short-duration extreme rainfall event are often the main cause of sudden and catastrophic floods (Kieffer and Bois, 1997). Generally, extreme rainfall events of relatively short duration appear to have the most impact in terms of damage inflicted. For instance, Panthou et al. (2014) indicated that Ouagadougou (Burkina Faso) experienced dramatic inundation on 1 September 2009 associated with 263 mm of rainfall recorded over 10 h. From a modelling point of view, any change in the temporal characteristics of an intense rain event could impact the results of sewage and drainage system simulations, hence the need to analyse extreme rainfall events at sub-daily or hourly timescales. Extreme rainfall characteristics have already been studied at different time intervals–from day to hourly and sub-hourly sampling of available data–for certain regions outside Africa, particularly over Lorraine, France (Estorge et al., 1980) and over Barcelona, Spain (Casas et al., 2004, 2010). These studies investigated the behaviour of intense extreme rainfall events at sampling intervals between 5 min and 24 h.

The present study addresses two well-known mesoscale sites located in different climatic zones. The study relies on numerous gauge stations distributed throughout these sites during the AMMA (African Monsoon Multidisciplinary Analysis) measurement campaign and CATCH (Couplage Atmosphere Tropicale Cycle Hydrologique) experiment to identify extreme rainfall event characteristics at sixteen different time intervals from 5 min to 24 h. In particular, we utilized the 5-min recorded rain series to classify extreme rainfall events based on specific sampling durations corresponding to the scale of the physical processes involved in those events. This study compares the characteristics of extreme rainfall events in two climatically different areas of West Africa (the Sahel and the Soudanian zone). While current research may continue to map extreme rainfall characteristics across West Africa (Panthou et al., 2012), it is worth noting that precipitation events in this region are characterized by strong climatic and local variability. This spatial variability could therefore impact the characteristics of extreme events from one area to another. As a result, an accurate statistical analysis of West African extreme rainfall events requires that investigations be based on climatic zones.

The following section describes the study areas, the rainfall dataset, and the methodology used to differentiate between rainfall events and identify extreme values. In Section 3, a statistical analysis of extreme events is performed, and the event characteristics are discussed to determine their possible origins. Finally, Section 4 summarizes the primary results of this study and suggests additional studies to be carried out based on this paper.

2. Data and methodology

The international research program known as the African Monsoon Multidisciplinary analysis (hereafter referred to as AMMA) deployed rainfall gauges across three well-known mesoscale sites in West Africa with the aim of better understanding the links between the hydrological cycle and climate variability at this scale (Lebel et al., 2010, see their Fig. 3). The sites studied are: the AMMA-CATCH Niger site located in the Sahel region of Niger (1.6–3.2°E; 13–14°N), the Malian Gourma site located in Mali (2–1°W; 15–17°N) and the AMMA-CATCH Benin site–formerly called the Hydro-meteorological Observatory of the Upper Ouémé Valley (hereafter OHHVO)—located in the Soudanian zone in North Benin (9–10.4°N; 1.5–3°E). Only the data from the AMMA-CATCH Niger and Benin meso-sites, which include well-instrumented super-sites, were used in this study.

2.1. Description of the study areas and data

The AMMA-CATCH Niger area is approximately 16,000 km^2 and is located between 1.40°E and 3°E longitude and 13°N and 14°N latitude (Fig. 1). The rain gauge network in this region extends into the neighbouring region of Niamey. Originally, the network was set up during the EPSAT (Etudes des Précipitations par SATellite)-Niger experiment, which aimed to characterize the variation in precipitation in the Sahel at a relatively wide range of spatial and temporal scales, including the convective cell scale, to contribute to the development and validation of satellite-based rainfall estimation algorithms (Lebel et al., 1992). The AMMA-CATCH Niger study area is located in the core of the Sahel region and is dominated by two seasons, the dry season, which runs from October to May, and the rainy season, which runs from June to September. Rainfall accumulation oscillates between 450 and 600 mm per year. Throughout the paper, this site will be referred to as the EPSAT zone.

The AMMA-CATCH Benin (9–10.4°N; 1.5–3°E) area (OHHVO) is characterized by a Soudanian climate. The unimodal rainfall regime extends from mid-March to the end of October (Yabi and Afouda, 2012) and intensifies during the months of July and August. This region is located in a climatic transition zone, with a humid climate regime to the South and a relatively dry regime to the North. The average annual rainfall is approximately 1200 mm. Initially equipped with daily rain gauges, the AMMA/CATCH programs strengthened the network of gauges in this area to include tipping bucket gauges and other equipment (i.e., radars, disdrometers, piezometers, limnigraphs, etc.). The purpose of such equipment was to study the life cycle of precipitating systems at the mesoscale, and their impact on watersheds at the local scale.

Across these study areas, rainfall measurements were taken from tipping bucket gauges with a 0.5 mm capacity, which provided a suitable temporal description of rainfall rates in the regions (Depraetere et al., 2009). This study was conducted using precipitation data from 2000 to 2010 recorded by each station in the EPSAT area (Niger) and from 1998 to 2010 in the OHHVO zone (Benin). The number of data points varied from year to year, with an average of forty (40) stations contributing to the EPSAT dataset and forty two (42) stations contributing to the OHHVO dataset, as outlined in Table 1. The available raw data used in this paper included 5-min rainfall records gathered from the two mesoscale networks for all stations and all years considered in this study. Other sub-hourly, hourly and daily sampling durations (10, 15, 20, 25, 30, 35, 40, 45, 50, 55, 60, 120, 360, 720, 1440 min), which constituted relevant scales for this work, were subsequently defined and new samples were taken to determine the cumulative rainfall for each of the chosen intervals.

2.2. Methodology

The main purpose of this study is to analyse, characterize and classify extreme rainfall events across the selected study areas. The extreme values theory provides two methods for sampling these extremes: the Block Maxima Analysis (BMA) and the Peak Over Threshold (POT) method (Panthou et al., 2012, 2014). The latter approach consists of defining a threshold and selecting all variable X occurrences that surpass this threshold, as shown in the work of Liebmann et al. (2001), where variability in daily extreme precipitation events was assessed. The BMA method defines blocks of n occurrences of the random variable X followed by the selection of the maximum value within each block. For example, when daily rainfall is set as variable X, the daily data for a one year period

Table 1
Number of stations per year on the EPSAT (Niger) (top) and OHHVO (Benin) (bottom) Observing sites.

Year	2000	2001	2002	2003	2004	2005	2006	2007	2008	2009	2010
Number of stations	30	30	30	30	30	30	30	57	57	57	55

Year	1998	1999	2000	2001	2002	2003	2004	2005	2006	2007	2008	2009	2010
Number of stations	13	30	37	37	47	43	43	36	52	54	56	44	44

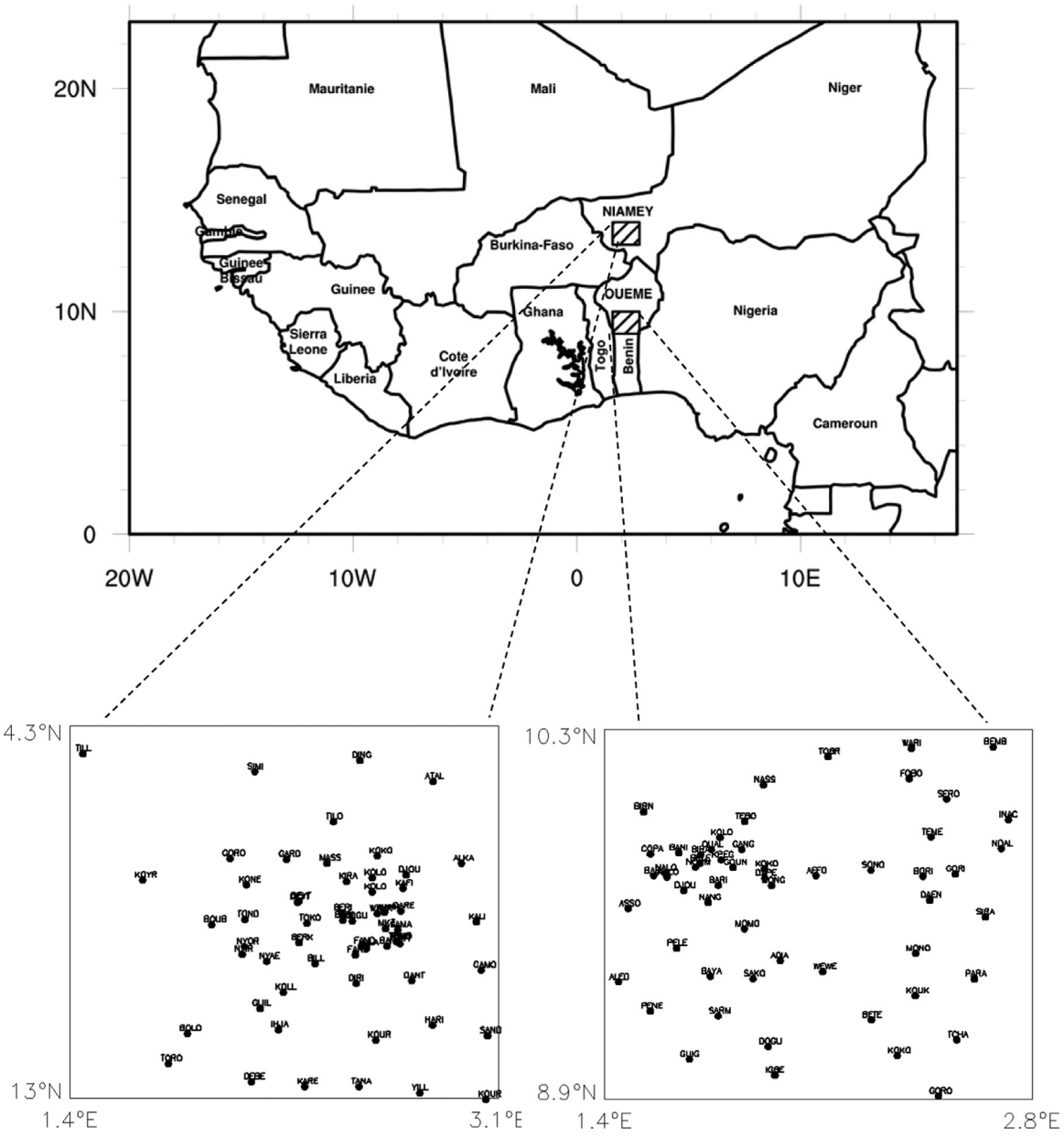

Fig. 1. Location of AMMA-CATCH mesoscale observing sites (hatched areas) which data were used in the study. Bottom figures illustrate the rain gauges networks installed on these regions: (left) the sahelian region named EPSAT in the text, (right) the soudanian OHHVO area.

would be grouped as a single block. The vector of maxima Z, defined as the annual maximum daily rainfall value within each block, would be written as follows (Panthou et al., 2012, 2014):

$$Z=\{Z_1,\ldots,Z_l\}$$
$$=\left\{\max(X_1,\ldots,X_n),\ \max(X_{n+1},\ldots,X_{2n}),\ldots,\max\left(X_{p-n+1},\ X_p\right)\right\}$$

where l is the number of years considered, n is the days in one year, and p is the total number of days during N years.

The BMA method has been adopted in the present work; however, unlike in Panthou et al. (2012, 2014), where the blocks consisted of daily rainfall data per year, here each block represents a set of rainfall events. This allowed us to overcome the relatively small number of years studied and provided a sufficiently large number of sample blocks whose maximum distributions could then be approximated using GEVs (Generalized Extreme Values). This methodological approach has been used in the literature to distinguish rainfall events based on criteria related to convective systems over the study areas. However, because of the present study's scope, we modified the existing criteria somewhat. As a result, each event was categorized according to the sample time intervals mentioned above to statistically analyse each event and identify those with extreme characteristics. In the final step of the approach, we classified the selected extreme events using an objective cluster analysis. As discussed later in this paper, this separation technique requires the application of additional criteria based on the study area.

2.2.1. Determination of rain events

Typically, rainfall events are used to connect rainfall measured on the ground to individual convective cloud systems. However, while these events help us understand the relationship between precipitating systems and rain measured on the ground, the determination of this relationship remains subjective. It depends not only on the researcher's point of view and goals but also on the scale of the observations made and the type of data available. For

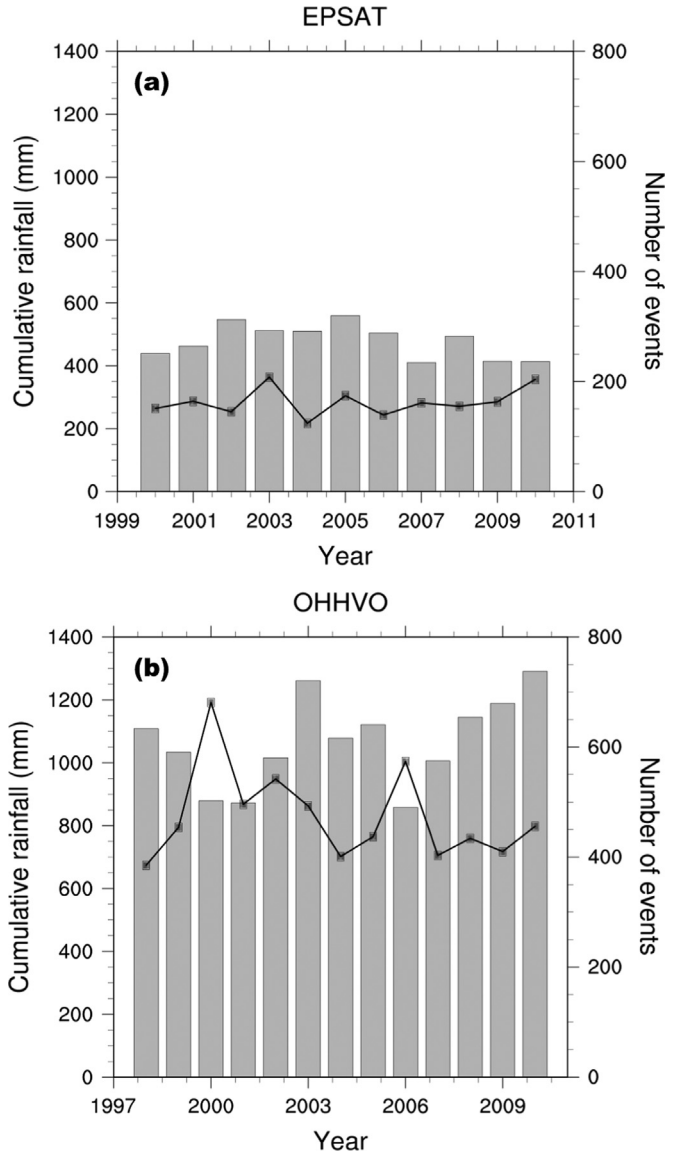

Fig. 2. Mean annual rainfall totals and number of rainfall events per year observed on the study areas: (a) EPSAT area, (b) OHHVO zone. The histograms and curves represent rainfall totals and associated number of events, respectively.

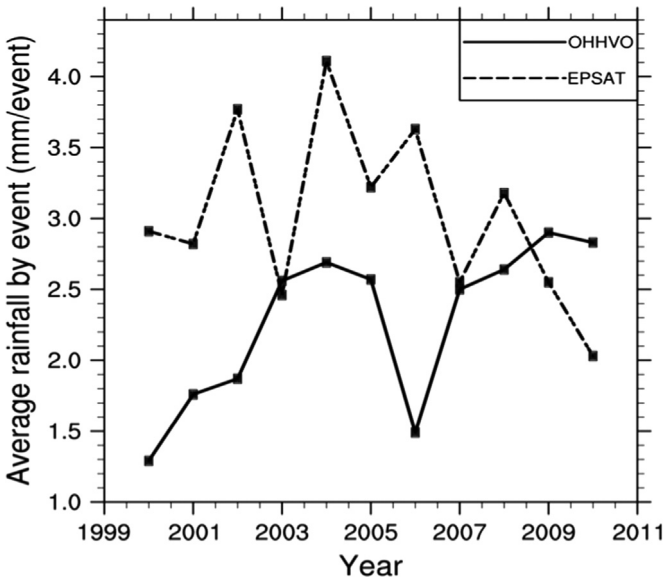

Fig. 3. Average annual rainfall per event for each year considered over EPSAT and OHHVO area.

Table 2
Fitting parameters of the GUMBEL distribution theoretical model on maxima rainfall sampled for duration between 5 min and 24 h and related Mean Absolute Deviation (MAD) values: (top) EPSAT area and (bottom) OHHVO area.

Durations (min)	Gumbel parameters		MAD (mm)
	a	b	
5	6.62	4.82	0.86
10	10.10	7.44	1.28
15	12.74	9.57	1.67
20	14.74	11.00	1.77
25	16.94	12.70	2.19
30	18.09	13.69	2.31
35	19.79	14.72	2.50
40	20.72	15.67	2.51
45	21.45	16.08	2.47
50	22.16	16.76	2.58
55	22.51	17.09	2.63
60	22.76	17.57	2.59
120	25.54	20.51	1.86
360	25.54	20.51	1.86
720	25.54	20.51	1.86
1440	25.54	20.51	1.86
5	7.40	6.18	0.71
10	11.07	8.57	1.10
15	13.91	10.44	1.70
20	16.19	12.20	1.97
25	18.34	13.61	2.27
30	20.25	15.09	2.42
35	21.87	16.23	2.63
40	22.91	17.13	2.52
45	24.25	18.29	2.82
50	25.19	18.91	2.91
55	25.83	19.56	2.96
60	26.57	20.04	2.99
120	30.38	23.57	2.87
360	32.28	25.73	2.45
720	32.22	25.75	2.40
1440	32.22	25.75	2.40

example, meteorologists use radar and satellites images to associate individual rain events with atmospheric disturbances limited in time and space. In contrast, hydrologists use rain gauge networks to define rain events by their hyetographs, which quantify the amount of water measured (volume event), peak intensity, and duration of each event.

In this study, we analysed the data from a hydrological point of view because the data were primarily acquired from rain gauges. In this context, the definition of each rainfall event depended on whether we relied on a single gauge ('point aspect') or an ensemble of gauges such as the dense networks across the EPSAT and OHHVO areas ('spatial aspect') to identify the event. Given data from a single station, Smith and Schreiber (1973) and Bouvier (1986) indicate that a rain event can be characterized by two parameters: (i) a time criterion associated with the minimum duration between rainfall occurrences that can be used to differentiate a prior rain event from the next, and (ii) a quantitative criterion associated with a rain depth threshold, below which the event is considered null.

To reflect the dynamics of precipitating systems, it is important to consider the 'spatial' aspect of convective systems, particularly because the same event may be detected by many gauges at different times. To this end, D'Amato and Lebel (1998) added a criterion related to the spatial continuity of a rain field in their study of the climatology of Sahelian rainfall events, expanding on the

two parameters previously mentioned by Smith and Schreiber (1973) and Bouvier (1986). This third criterion is represented by the minimum percentage of observation stations affected. This addition of a "spatial" aspect to the definition of a rainfall event is therefore well-suited to the type of data gathered from the two gauge networks used in the present study. According to Mathon et al. (2002), because the area covered by the network (approximately 15,000 km^2) and that covered by a given convective system are comparable in size, the probability of observing two distinct precipitating systems simultaneously within the study area (EPSAT Niger, also known as the Niamey square degree area) is relatively negligible. This same area, along with a second area of a similar size (OHHVO) was analysed in the present study. Thus, we define a rain event using the following criteria:

- The duration of null precipitation separating two independent rainfall events (in this study, a gap of 30 min was chosen);
- The rain depth threshold (1 mm) below which an absence of rain was assumed;
- The percentage of gauges that recorded an event's rain depth equal to or greater than 1 mm.

In terms of the latter criterion, a rainfall event was quantified if it was observed by at least one gauge or more. We chose this value because a rainfall event may have an extreme nature while being highly localized, as argued by Panthou et al. (2012). In addition, one of this study's objectives is to identify as precisely as possible those groups of rainfall events that originate locally as well as the disturbances that cause such extreme rainfall. Based on these criteria, multiple spatial and zonal rainfall events were identified. The number of these events varied from year to year. The number of rainfall events and the annual averaged cumulative rainfall per year is shown for both the EPSAT and OHHVO areas in Fig. 2. These major events were distinguished from a group of individual episodes recorded at each gauge by identifying the beginning of the zonal event as the date of the first tipping bucket rain gauge record. In this study, this date corresponds with the first date from which the lowest amount of precipitation across the network was observed. The end of the event is the last date during which precipitation was recorded prior to no precipitation registering across the network.

Fig. 2 shows the high inter-annual variability of precipitation in both study areas and reveals that no correlation exists between the number of rainfall events observed annually and the cumulative annual averaged precipitation. These results confirm those obtained at the regional scale and indicate the existence of a latitudinal gradient related to average annual precipitation, where total rainfall is greater in the Soudanian region than in the Sahel area. However, in terms of the efficiency of precipitating systems (the ratio of average annual cumulative rainfall compared to the total number of rain events), the average annual rainfall produced by rain events (Fig. 3) indicates that convective systems over the EPSAT area produced more precipitation than those across the OHHVO area, even though there were fewer of the former. Averaged annually, each event produced 3.02 mm of rain in the EPSAT area, whereas 2.33 mm of rain was produced per event in the OHHVO zone. However, from 2009 onward, this trend was reversed; yet this change did not appear to impact the occurrence of floods and inundations in the two regions. For instance, in 2009 an unprecedented amount of rainfall, 263 mm in 10 h (Panthou et al., 2012, 2014), occurred in Ouagadougou, which is located in the same climatic region as Niamey (Sahel central), and inundated the area. Similarly, historical floods overflowed the banks of the Niger River (Panthou et al., 2014) in 2010 and 2012, resulting in dramatic, disastrous socioeconomic impacts to the people living near the river. According to the National Meteorological Service, 2010 was marked by inundation across Benin, including the OHHVO area. Yabi and Afouda (2012) noted the increase in extreme rainfall in Benin during 2009 and 2010.

In general, Mathon et al. (2002) and Depraetere et al. (2009) revealed that the average cumulative rainfall per event was stronger in the Sahel region than in the Soudanian zone (10.2 mm versus 9.7 mm per event) through their studies of the same EPSAT zone from 1990 to 94 and 1996–99 and that of the OHHVO area using 1999–2006 rain gauge data, respectively. The difference between their results and the present study is a reflection of the criterion used to define a zonal event – the percentage of stations that recorded a rain depth greater than the 1 mm threshold–and also the definition of the minimum average rainfall in the OHHVO area (1 mm here versus 5 mm in Depraetere et al.). In this study, we quantified a rain event when at least one station registered its occurrence to account for localized rainfall events, whereas Mathon et al. and Depraetere et al. relied on a 30% threshold to define a zonal event. As a result, we identified more zonal rainfall events and thus lower efficiencies within precipitating convective systems.

Regardless of the variations in precipitating systems' efficiencies from one region to another, twelve member states within the West African region were victims of inundations in 2009. As a result, there is a desire to understand the links between rainfall and floods or inundations on the one hand and extreme rain events and inundations on the other. Investigating these links is not within the scope of the present study; however, we do identify the characteristics of extreme rainfall events and the origins of meteorological disturbances that cause such exceptional events in the following sections.

2.2.2. Differentiation of rainfall events and calculation of return periods

The hyetographs for previously determined individual rainfall events at each gauge were revisited using sixteen sub-hourly, hourly and daily sampling time intervals: 5 min, 10, 15, 20, 25, 30, 35, 40, 45, 50, 55, 60 (1 h), 120 (2 h), 360 (6 h), 720 (12 h), 1440 min (24 h or 1 d). Maximum rainfall per event was then extracted from each gauge for the relevant durations. By considering independent rainfall events for all years using the BMA method, we obtained significantly large datasets per sampling duration. A statistical analysis of these different maximum rainfall samples for durations between 5 min and 24 h was performed to determine the reliability of the extreme nature of these maximum values. We also aimed to detect specific or systematic anomalies in the data series. In the present case, because of the extreme nature of the data (we only considered the maximum value of each rainfall event given the sampling interval), conventional methods for detecting anomalies in the data series, including the analysis of the cumulative residuals' regression between a reliable reference variable and the test variable, could not be applied. For this reason, we graphically fitted each maximum rainfall value derived using Gumbel's statistical distribution law for each sampling duration to prejudge the data's reliability. The Gumbel distribution is one of three of the most used extreme distributions that constitute the generalized extreme values' (GEV) distribution conventionally employed in frequency analyses of precipitation data in general (Pilon et al., 1991) and in West African extreme rainfall events in particular (Goula et al., 2012; Panthou et al., 2012, 2014).

In a GEV frequency analysis of maximum rainfall, the distribution behaviour description is based on the difference or distance between the ideal and asymptotic behaviour of a theoretical law and the actual behaviour of a physical phenomenon observed in frequency ranges and necessarily distant from the asymptote, where the homogeneity of the events is not verified and atmospheric processes are disrupted by natural thresholds.

The Gumbel cumulative distribution function (CDF) is given by

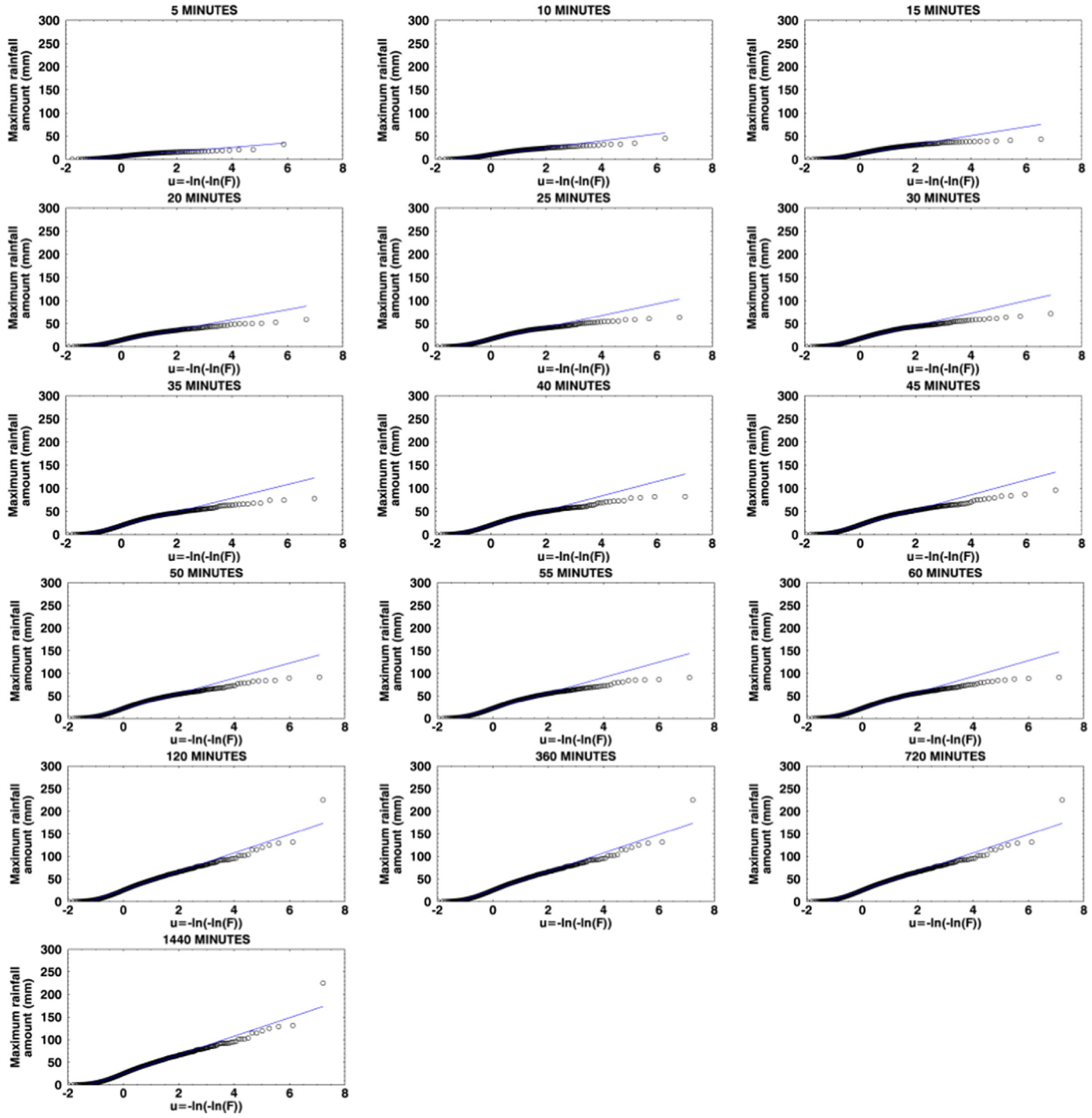

Fig. 4. Fitting of maximum rainfall drawn from Gumbel distribution for various sampling durations for Niamey (EPSAT) square degree case.

the relationship:

$$F(x) = exp\left(-exp\left(-\frac{x-a}{b}\right)\right) \quad (1)$$

where $u = \frac{x-a}{b}$ is defined as the reduced Gumbel variable; a and b are the parameters of the model; and the variable x is the random rainfall maximum variable. The distribution is then expressed in the following way:

$$F(x) = exp(-exp(-u)) \; and \; u = -ln(-ln(F(x))) \quad (2)$$

Simulations have shown that, for the Gumbel distribution, it is wise to use the Hazen (1914) empirical formula given by the equation:

$$F(x) = \frac{r-0.5}{N} \quad (3)$$

In this relationship, r is the rank of the observation x and N represents the sample size of the observed maxima series. This allows access to the reduced variable u, which is linearly related to the maximum rainfall value (x). Subsequently, a linear fit using a 'robust' least absolute deviation (LAD) technique (Thanoon, 2015) determines the two Gumbel parameters a and *b* (as shown in Table 2 for each sampling interval), also known as the modal or

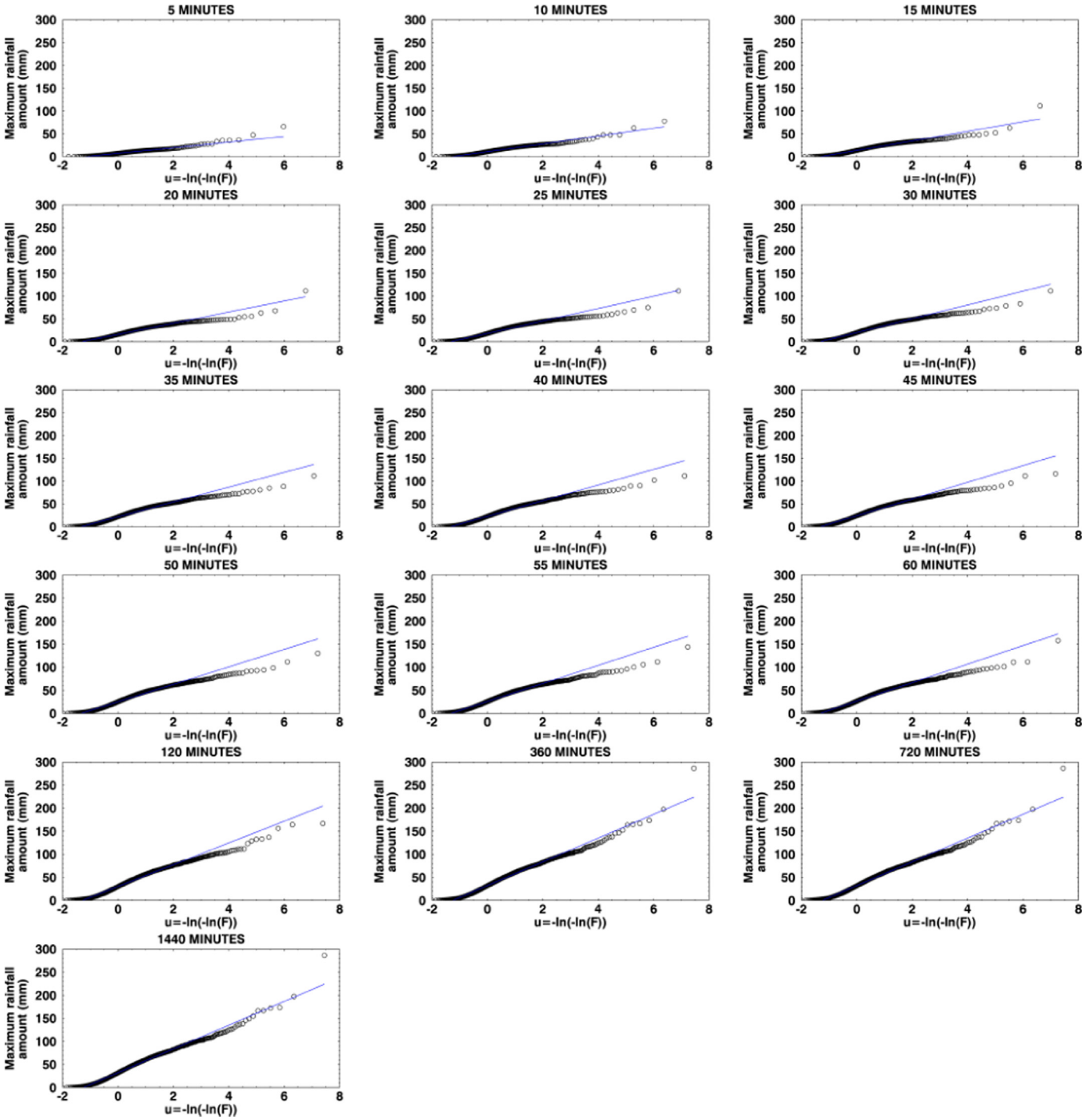

Fig. 5. Idem Fig. 4, but for OHHVO square degree area.

most probable value and Gradex (for exponential gradient), respectively. The robust LAD regression is suitable in cases where abnormal values are present because it has been found to be less sensitive to outlying data than an ordinary least square regression (Thanoon, 2015).

This approach is shown graphically in Figs. 4 and 5**,** which highlight the ability of the Gumbel CDF to model series of maximum values for each discrete time interval. The observed values aligned well within the regression, or the theoretical line for the lowest Gumbel reduced variable "u" values. However, an offset was observed for the highest values using the same parameter. This offset was reduced for longer sampling durations. The resulting low mean absolute deviation (MAD in Table 2) indicates that the Gumbel extreme values distribution can be used to draw the observed rainfall maxima series. Presumably, this shows that there are no erroneous rainfall values within the different samples, at least for certain discrete durations (15 min to 1 h) where the values that were observed furthest from the theoretical curve are negligible with respect to the entire sample. These values cannot be considered erroneous because the samples for the same rainfall events identified for durations less than 15 min or greater than 1 h show that the differences between the experimental points and the theoretical curve are low.

A calculation of the cumulative frequency F in the literature

(Casas et al., 2004) has shown that it is possible to determine the return period *T*, a theoretical average duration within a given year that separates two occurrences of a given phenomenon. The return period of an event is defined as:

$$T = \frac{1}{1 - F}. \quad (4)$$

Thus, for a given return period *T* of 1, 2, 5, 10, 20, 50, 100 years, when the frequency F is known (from Eq. (4)), the maximum rainfall value for a given discrete time interval is determined by combining Eqs. (2) and (4) and the relationship $u = \frac{x-a}{b}$.

The relationships thus obtained between the maximum rainfall intensities, the sampling duration and the frequency of intense rainfall are commonly known as Intensity-Duration-Frequency (IDF) curves. These IDF statistics characterize rainfall by giving the occurrence probability for various rainfall intensities and different sampling durations in a given place. In this study, rainfall rates with return periods of 1, 2, 5, 20, 50, 100 years were calculated by applying an extreme value analysis to the observed data. Fig. 6 shows the IDF curves for the EPSAT and OHHVO study areas. An increase in the maximum rainfall intensity was noted for certain return periods and for a given sampling duration over both study areas. For a fixed return period, the figures indicate a decrease in the maximum rainfall intensity as the sampling duration increases. Given a 5-min sampling interval, the IDF curves show that a maximum rainfall intensity of 4.4 mm/min has a 10-year return period in the OHHVO area but a 100-year return period over EPSAT area. Similarly, for a 1-day (1440 min) sampling interval, a maximum rainfall intensity of 0.06 mm/min with a return period of 10 years was found for the OHHVO zone while a 50-year return period was found for the same interval and intensity over the EPSAT area. Thus, we can conclude that in the Soudanian OHHVO zone, the occurrence of extreme rainfall rates is higher (has a very short return period) compared to EPSAT rainfall events. This shows the stress suffered by the OHHVO area in terms of extreme rainfall events, which we will see reflected in the determination of extreme events in these regions over the study period. Finally, an analysis of this figure reveals a stronger variability in the maximum rainfall intensity as the sampling duration is decreased in the two areas. These results are similar to those obtained by Casas et al. (2004). However, this variability is stronger over the Soudanian zone than the Sahelian area.

The maximum values analysis appears to both characterize the probability and magnitude of events that are more extreme than any others within a given data series (Coles, 2001). The analysis also provides an estimate of a suitable threshold for the identification of extreme rainfall events and their return periods. Estimates of extreme rainfall recurrence intervals are indispensable to the construction of infrastructure that is able to withstand recurrent inundations. To this end, Intensity-Duration-Frequency curves provide a means by which estimates of the critical intensity for a given return period can be made. In the next section, we use IDF curves to determine the extreme rainfall events that occurred within the EPSAT and OHHVO areas during the study period.

2.2.3. Determination and classification of extreme rainfall events

Determining extreme rainfall events is relatively difficult given the possible variations in their definition from area to area and study to study. Liebmann et al. (2001) characterized an extreme rainfall event at a station where the daily precipitation exceeded a certain percentage of the seasonal or annual climatological mean total precipitation. In their study, the thresholds of 3, 4, and 5% were tested based on an assumption that extreme rainfall was relatively rare. Casas et al. (2004, 2010) argued that a rainfall event

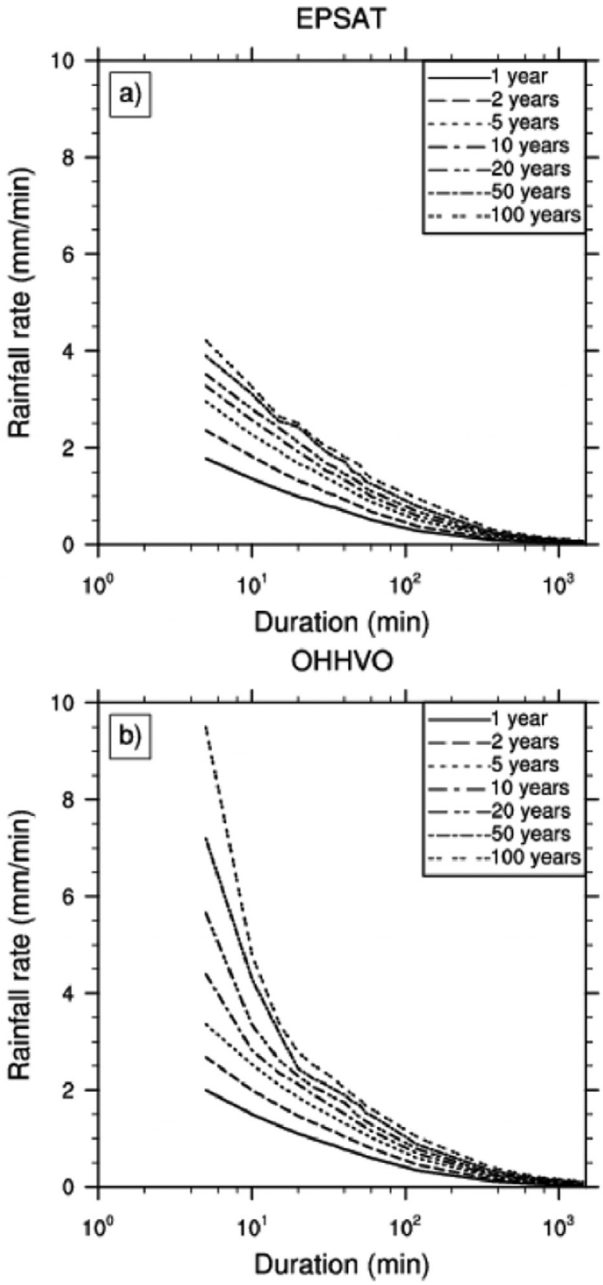

Fig. 6. Intensity-Duration Frequency curve showing the average maximum rainfall rate corresponding to each time interval, calculated from Gumbel theoretical frequency distribution: (a) the EPSAT (Niger) area and (b) OHHVO (Benin) area.

is extreme when the amount or intensity of the rain (amount or intensity above a defined threshold) over a given time interval has a return period greater than or equal to 5 years for any sampling duration between 5 min and 24 h. Casas et al.'s (2010) data were configured similarly to ours. Namely, both studies reduced the number of stations (23 for Casas et al. versus a variable number of stations from one year to the another up to 57 stations in the present study) and years (8 years for Casas et al. versus 11 or 13 years depending on the area of study in the present work) measured, particularly when compared to the long series data (40 years of daily data) recorded by more than 200 rain gauges in Liebmann et al. (2001). For this reason, we adopted the definition in Casas et al. Based on a 5-year return period, they modelled the corresponding IDF curve using the following relationship:

$$I(t, T) = \frac{19 \log T + 23}{(13 + t)^{0.87}}. \quad (5)$$

where t indicates a sampling interval from 5 min to 1 d and T is the return period (here, equal to 5 years). The choice of a 5-year return period is justified by the fact that the occurrence of an extreme event several times a year at a given location would result in the development of infrastructure to mitigate its potential damage. The same event occurring once every 5 years would inflict more damage because fewer mitigation measures are likely to be in place while an event with 50-year return period is not of interest to many decision makers. In this study, we used Eq. (5) to re-calculate the rainfall intensities or cumulative rainfall for a 5-years return period and each sampling interval. The theoretical IDF curve obtained from Eq. (5) and the corresponding observed values from our data are shown in Fig. 7. The comparison of IDF curves derived from our data with the parametric estimates in this figure indicate that the theoretical IDF model from Casas et al. (2004) provides a good threshold for selecting extreme rainfall events, especially because the root-mean-square-error (RMSE) values observed between the observed IDF values and those derived from the theoretical model are relatively low (0.13 mm/min for the Sahelian zone and 0.12 mm/min for the Soudanian zone). Although Casas et al.'s theoretical IDF model does not fit our data perfectly and likely is not intended to determine all extreme rainfall events, it is an indication that the extreme behaviour of the selected events is obvious, particularly because this model constitutes an upper limit for the IDF derived from our data. Therefore, for each sampling interval in the present study, we considered the theoretical rainfall quantity as the threshold beyond which any observed maximum rainfall value would be regarded as extreme. In other words, a rainfall event was classified as extreme when it had an intensity or a depth equal to or greater than the theoretical threshold with a return period equal to or greater than 5 years for at least one of the durations between 5 min and 24 h. Thus, at each station, all rainfall events greater than or equal to the values given by the theoretical model described in Casas et al. (2004) for one or more sampling intervals used in this study have been identified as exceptional or extreme.

For West Africa, Mathon et al. (2002) and Depraetere et al. (2009) have outlined the existence of various convective systems with different characteristics at different spatial scales (local, meso and synoptic). These different atmospheric disturbances at various scales may be the causes of extreme precipitation. To investigate the origin of extremely intense rainfall events, Casas et al., (2004, 2010) proposed classifying these events according to the temporal similarities present during their evolution. The event classification method is based on the cluster analysis approach that, according to Djomou et al. (2009), is part of the most commonly used methods for rainfall classification. The methodology relies on the concept of Euclidean distance in a virtual (non-physical) space and has sixteen (16) dimensions corresponding to sampling durations ranging from 5 min to 1440 min (or 1 d) used to differentiate between rainfall events. Thus, at each station, each previously determined extreme rainfall event has 16 rainfall rates as measured for each sampling interval. These values are considered the coordinates of a given extreme rainfall event in the sixteen-dimension virtual space. The selection of extreme rainfall event clusters occurs through the calculation of the Euclidean distance between each event in virtual space. The lower the Euclidean distance between two rainfall events, the more similar they are. In practice, the UPGMA (Unweighted Pair Group Method using Arithmetic average) algorithm classification used here is composed of five main steps (Djomou et al., 2009), which ultimately will allow us to cluster rainfall events in the form of a hierarchical dendrogram.

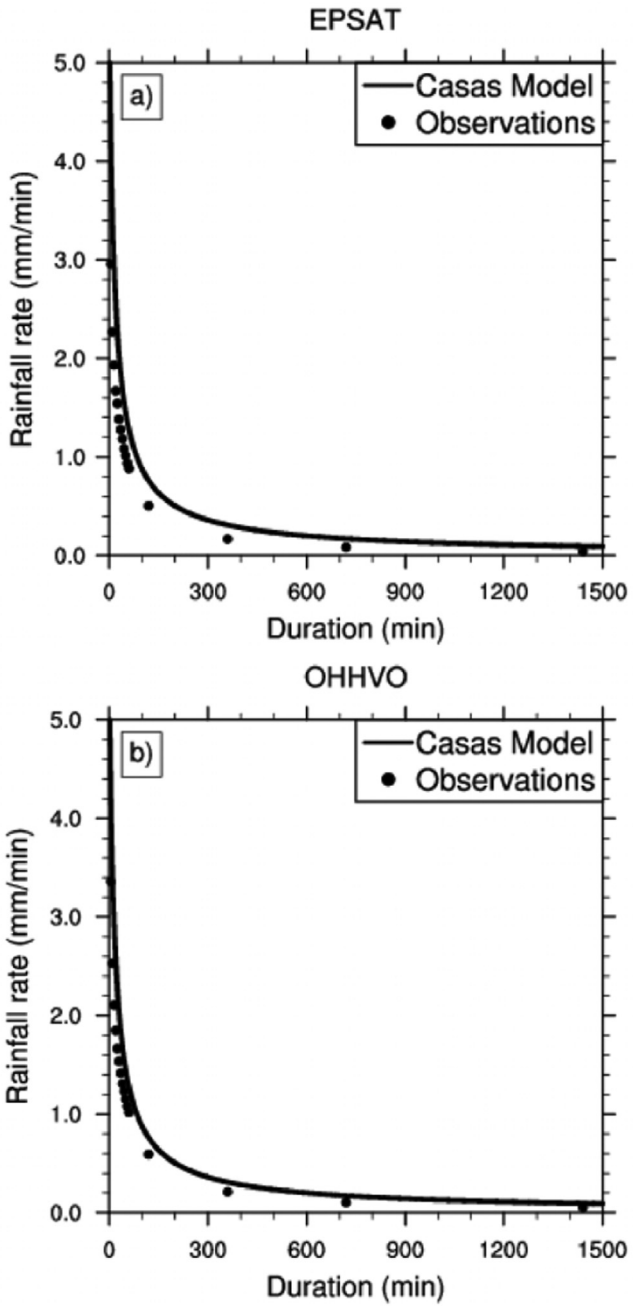

Fig. 7. Comparison of 'Observed data' and Casas et al. (2004) model IDF (Intensity-Duration-Frequency) curves for a 5-years return period: (a) EPSAT zone and (b) OHHVO area.

The steps are as follows: (1) the Euclidian distances between all pairs of extreme rainfall events are calculated in the 16-dimension virtual space; (2) based on a distance criterion, the events are listed in the same group or separated into different groups, thus forming new entities; (3) the distances between all new entities or groups is recalculated (The distance between two entities or clusters is defined as the average distance for all pairs of 'objects' between each cluster unweighted by the number of objects in each cluster); (4) steps (2) and (3) are repeated until all entities are merged into a single cluster; (5) a distance threshold is applied to the dendrogram thus obtained to deduce different event groups (clusters). Subsequently, each group is assigned a supposed origin according to the common features of its elements in the virtual Euclidean space.

Generally, extreme rainfall episodes are expected to be

commonly associated with the synoptic system in which the episode is set. Sometimes, however, the general pattern does not sufficiently explain the total amount of rainfall and the location of the highest convective activity associated with the disturbance. Doswell (1987) argued that mesoscale processes may at times be sufficient to initiate deep convection in environments that may be marginally favourable for convection. Therefore, it appears necessary to look for sub-synoptic mechanisms that could focus and trigger extreme rainfall events. In the course of this paper we have outlined three meteorological scale (local, meso and synoptic scales) analyses which must be carried out when undertaking an in-depth study of extreme rainfall episodes. The usual method of defining scales of processes involved in extreme rainfall events is based on previous studies from Orlanski (1975) and Thunis and Bornstein (1996), which discussed various scale definitions using characteristic spatial and temporal scales for a variety of atmospheric processes. However, this approach seems to be rather arbitrary with regard to the determination of the beginning and end of the scale categories (i.e., the location of the interfaces between scales). By synthesizing these previous works and Casas et al. (2004), we defined local scale, mid-mesoscale, large mesoscale and synoptic scale contributions corresponding to duration intervals 1*h* (less than an hour),1 – 2*h*, 2 – 6*h* and 6*h* (more than 6 h). These scales were used to categorize extreme rainfall events according to their severe behaviours over typical durations. Although this study did not seek to describe a direct correlation between extreme rainfall events and atmospheric features, the advantage of this type of study is that it permits an evaluation of distinct scales of processes within extreme rainfall events. Therefore, these results could be included in prediction models where accurate rainfall monitoring is an ongoing issue.

3. Results and discussion

3.1. Statistical analysis of extreme events

For the period analysed, 32 extreme events exceeding at least one theoretical rainfall amount threshold occurred in the EPSAT zone, including 22 actual 'spatial' rainfall events, as summarized in Table 3. In this table, rainfall values in bold correspond to values that have exceeded the 5-year return period (or that have exceed the corresponding 5-year return period fixed threshold derived from the theoretical model of Casas et al., 2004) for some of the discrete time intervals considered. Therefore, these values indicate the duration over which the various events have exhibited extreme behaviour. In the OHHVO zone, 75 spatially extreme rainfall events were found to yield 90 extreme cases where rainfall amounts exceeded the threshold for at least one sampling interval (Table not shown). Although the causality between extreme rainfall events and inundations cases is not yet well understood, it is relevant to note that at regional scale, a total of 89 inundation cases occurred across all of the West African member states, where EPSAT and OHHVO zones are located, during nearly the same period (2000–2008). Based on the number of sampling intervals for which extreme events maintained their exceptional character, Table 3 (EPSAT, same as for OHHVO, which is not shown) shows that these events do not exhibit the same similarities and therefore are presumed to be of various origins. This suggests that they would likely be marked by different, more or less significant impacts.

The percentage of extreme events in relation to the total number of rain events that swept the EPSAT and OHHVO regions each year is shown in Fig. 8. The relatively low ($< 2.5\%$) proportions of rainfall events classified as extreme, which are consistent with the values identified over the central Sahel in Panthou et al. (2014), are highly variable within the same area from one year to another and from one area to another. Although clear interannual variability can be seen, with both increases and decreases in frequency occurring depending on the year, three distinct periods were observed: (i) the period 2000–2003, which was characterized by heterogeneous extreme events with a greater average ratio in the Soudanian region, (ii) the period 2004–2008, which was marked by a clear distinction between the ratio of extreme events in the EPSAT and OHHVO areas and where proportions were relatively higher in the Sahelian zone (EPSAT), and (iii) the period 2009–2010, which indicated a greater ratio of extreme events in the Soudanian zone. These results clearly show both the high spatial and temporal variability of extreme rainfall events as well as most precipitating systems in West Africa, as highlighted by several previous works (Depraetere et al., 2009; Mathon et al., 2002). They also indicate how difficult extreme events are to predict and bring to the forefront the importance of analysing extreme rainfall events based on climatic area.

3.2. Characteristics of extreme rain events

Based on their similarities, the listed extreme events were classified into various groups and associated with certain rainfall process scales according to common characteristics within each group in virtual Euclidean space. The analysis of meteorological phenomena scales (local, mesoscale or synoptic scale convective systems), which lead to such exceptional events and their interaction, was performed based on sampling duration as suggested in several works (Mathon et al., 2002; Casas et al.,2004, 2010; Depraetere et al., 2009). The results of the classification obtained for each zone are shown in a dendrogram in Figs. 9 and 11. Although the interpretation of these diagrams remains simple, we had difficulty specifying the number of clusters to represent. To simplify this process, the shorter the linking branch between two events, the closer they are. As a result, we divided the dendrograms into 5 and 4 groups for the EPSAT and OHHVO areas, respectively, by drawing imaginary vertical lines (L_1 and L_2 in the figures) from a reference distance considered the minimum distance from which two events could be considered to have common characteristics. These imaginary lines allowed us to isolate certain rainfall events with similar characteristics from the cut off of nodes. At this stage, according to Casas et al. (2004), we classified the events in the dendrogram based on the desired number of groups. This was a rather random exercise, although the cluster analysis itself was objective because it was based on Euclidian distances. Other additional, more objective criteria were used to justify the choice of groups, the isolation of an extreme event, or the inclusion of an event in another group. Thus, for each extreme event considered in this study, we assessed its contribution in terms of rainfall amount (referred to as the ratio or proportion expressed in %) relative to the zonal mean total yearly precipitation amount of the considered area where it was observed. In a study devoted to the inter-annual variability of extreme daily rainfall in the State of São Paulo, Liebmann et al. (2001) defined a rainfall event as having being extreme when its daily total rain exceeds a threshold percentage of the average annual cumulative rainfall (climatological cumulative rainfall obtained by averaging the total annual rainfall for the period of data). However, to take into account the fact that rainfall can be extremely low, wet or normal in a given year relative to annual rainfall quantities, we chose the mean total annual rainfall per year (average of annual totals of all stations in the climatic zone considered). This approach was motivated by the wish to consider the extreme nature of events in the context of deficient, excessive or normal rainfall years when they occurred. Panthou et al. (2014) indicated strong extreme events in dry or moderately wet years, whereas some wet years may be

Table 3
Maximum rainfall in mm recorded for sampling time intervals from 5 min to 1440 min (24 h) for all extreme rainfall cases selected on EPSAT area (2000–2010). The values in bold indicate rainfall events exceeding the 5-year return period in some of considered durations.

Stations	Events	5 min	10 min	15 min	20 min	25 min	30 min	35 min	40 min	45 min	50 min	55 min	60 min	120 min	360 min	720 min	1440 min
	ddmmyy																
IRI	160800	14.6	**25.4**	**35.7**	**46.5**	**54.8**	**61.6**	**67.7**	**72.5**	**76.4**	**78.5**	**80.1**	**81.6**	**92.9**	**92.9**	**92.9**	92.9
DAREY	180800	13	**25.6**	**33**	**49.7**	**51**	**45.1**	**56.9**	**69.2**	**78.1**	**83.1**	**86.4**	**88.8**	**101.5**	**101.5**	**101.5**	**101.5**
BOUBON	140602	6.1	11.1	15.5	21.6	22.5	27.4	35.6	29.9	34	44.1	41.4	36.4	**91.5**	**91.5**	**91.5**	91.5
GAMONZO	300702	12.9	25	29.2	32	**41.2**	**49.1**	**55.6**	**60.5**	**64.7**	**67.9**	**70.3**	**72.1**	**92**	**92**	**92**	92
HARIKAN	060803	8.9	17.5	25.8	33.8	**39.9**	**43.2**	**46.2**	**50.5**	**56**	**62.2**	**66.8**	**75.7**	**119.5**	**119.5**	**119.5**	**119.5**
TANABER	060803	7.7	11.9	12.6	13.5	18.3	19	21.5	23.9	27.6	25.1	32.6	35.9	**96**	**96**	**96**	**96**
KOURESU	060803	10.5	19.4	22.7	33.2	35.4	**44.8**	**44.6**	**57**	**62.7**	**62.4**	**66.7**	**76.5**	**225**	**225**	**225**	**225**
KOYRIA	120903	**17.6**	**32.6**	**37.8**	**43.8**	**55.4**	**64**	**74.1**	**79.7**	**83**	**83.9**	**84.2**	**84.5**	**88**	**88**	**88**	88
GARDAMA	290404	13.2	**25.5**	**37.7**	**48.9**	**61**	**66**	**74.4**	**73.3**	**96**	**91.6**	**92.6**	**99.8**	**131.5**	**131.5**	**131.5**	**131.5**
MASSIKO	290404	9	17.8	26.1	29.6	37.1	31.2	45.4	**53.1**	**56.5**	**60.9**	**62.5**	**61.6**	**114.5**	**114.5**	**114.5**	**114.5**
IRI	290404	8.4	15.9	22.4	23.3	27.9	38.4	35.5	45.8	49.7	51.2	**56.2**	**61.6**	**125**	**125**	**125**	**125**
ORSTOM	290404	8.8	17.4	21.9	28.1	31.2	37.1	48.3	45.1	51.3	58.8	71.6	73.2	**129**	**129**	**129**	**129**
GOROUGO	290404	13.8	**25.8**	**38.3**	**36.9**	**47.7**	**59.7**	**65.1**	**70.8**	**75.4**	**78.3**	**80.7**	**82.1**	**86**	**86**	**86**	86
GUILAHE	070704	**16.8**	**25.9**	**35**	**44.1**	**51**	**57.9**	**64.9**	**68.5**	**70.2**	**71.2**	**72**	**72.6**	**85**	**85**	**85**	85
KOUREKO	200704	**16.2**	**32.1**	**37**	**52.9**	**58.9**	**61.3**	**62.6**	**63.5**	**64.1**	**64.5**	**65**	**65.5**	**76.5**	**76.5**	76.5	76.5
KOLLO	070605	**16**	**29.3**	**39**	**42.6**	**58.6**	**71.9**	**78**	**81.8**	**83.8**	**84.5**	**85.2**	**85.2**	**85.2**	**85.2**	**85.2**	82.5
IRI	170605	17.5	**30.1**	**38.2**	**59**	**55.6**	**48.7**	**66.2**	**78.8**	**86.9**	**89.5**	**90.7**	**91.3**	**91.3**	**91.3**	**91.3**	91.3
TORODI	020606	**32.5**	**45.2**	**47.4**	**50.1**	**53.5**	**55.7**	**55.7**	**55.7**	**55.7**	**55.7**	**55.7**	**55.7**	**55.7**	55.7	55.7	55.7
KOKORBE	230806	11.2	21	**32.1**	**39.5**	**47.1**	**47.4**	**62.8**	**68.8**	**64.4**	**64.8**	**66.3**	**71.1**	**86**	**86**	**86**	86
KOYRIA	100906	11.7	22.7	**31.3**	**44.2**	**42.9**	**50.7**	**61.5**	**72.2**	**79.2**	**82.6**	**85.5**	**87.4**	**91.6**	**91.6**	**91.6**	91.6
KONE_BERI	150707	**16.5**	**29.2**	**40.9**	**43.5**	**41.8**	**54.5**	**62.9**	**68.8**	**73.5**	**76.9**	**78.6**	**79.4**	**92.3**	**92.3**	**92.3**	92.3
TONDIBIAGOROU	220707	13.5	**24**	**33.7**	**39.7**	**52.4**	**46.6**	**67.9**	**71.3**	**67.3**	**68.1**	**68.8**	**70.1**	**82.4**	**82.4**	**82.4**	82.4
IH_JACHERE	040807	**16.4**	**32.4**	**43.4**	**50.7**	**63.9**	**65.9**	**66.1**	**67.5**	**70.4**	**78.7**	**82**	**83.8**	**94.6**	**94.6**	**94.6**	94.6
GOROU_GOUSSA	250608	10	18.7	27.7	35.3	39	41.3	**56.2**	**56.6**	**57.1**	**64.1**	**64.8**	**73.5**	**114.6**	**114.6**	**114.6**	**114.6**
KOYRIA	250608	8.6	16	19.6	24.6	28.5	34.4	40.3	44.6	48.6	55.2	**63.2**	**68.2**	**103.4**	**103.4**	**103.4**	**103.4**
BERKIAWEL	250608	9.2	15.6	19.2	26.6	29	36.8	36.7	39.4	44.7	48.3	**54.7**	**63.9**	**101.4**	**101.4**	**101.4**	**101.4**
TONDIBIAGOROU	250608	8.5	16.4	20	27.9	30.9	37.7	43.8	45.4	**51.9**	**54.2**	**60.8**	**61.7**	**95.2**	**95.2**	**95.2**	95.2
SIMIRI	180808	14.9	**27.8**	**33.4**	**46.3**	**53.8**	**54.7**	**56.6**	**56**	**72.8**	**74.6**	**81.2**	**85.5**	**92.2**	**92.2**	**92.2**	92.2
WANKAMA_PLATEAU	110908	12.5	23.2	30.9	**37.6**	**40.1**	**44.7**	**55.5**	**59.1**	**61.9**	**64.3**	**69.1**	**75.1**	**91.8**	**91.8**	**91.8**	91.8
SANDIDEY	110908	8.8	15.3	18.6	24.7	31.6	35.8	42.5	47	50.2	**54.2**	**58.6**	**61.5**	**101.7**	**101.7**	**101.7**	**101.7**
KOURE_SUD	080709	9.2	15.7	22.2	23.2	28.3	27.9	37.3	36.3	39.1	47.1	49.4	53.3	**91.5**	**91.5**	**91.5**	91.5
DEBEREGATI	060810	**17.1**	**21.7**	**37.7**	**35.4**	**39.8**	**46.8**	**50.4**	**51.2**	**68.3**	**72.9**	**75.1**	**77.4**	**79.4**	**79.4**	79.4	79.4

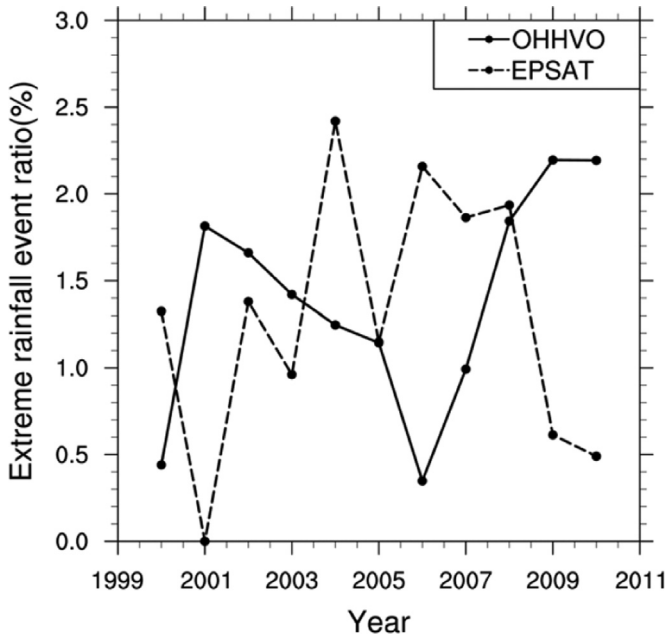

Fig. 8. Ratio of extreme rainfall events per year on EPSAT and OHHVO area.

characterized by few extreme events.

For the EPSAT area, we plotted the first virtual vertical line (L_1) and isolated two events from a third (Fig. 9). These events occurred on 06 August 2003 at the KOURESU station (KOURESU 060803) and 29 April 2004 at the GARDAMA station. This latter location (GARDAMA 290404) has the distinction of having intensities exceeding the threshold for the 5-year return period for almost every the sampling interval (Table 3). Such a result may indicate that the meteorological processes involved in this rainfall event cover several scales ranging from the local to the synoptic. Moreover, at the 5 responsive stations where the 29 April 2004 event exhibited high rainfall intensities, almost all sampling durations between 10 min and 24 h (GARDAMA: 10 min to 24 h, MASSIKO: 40 min to 24 h, IRI: 55 min to 24 h, ORSTOM; 2 h to 12 h, GOROUGO: 10 min to 12 h) revealed this spike. The somewhat complex character of this event is highlighted by the fact that the related extremes at the five aforementioned stations fell into different groups according to the dendrogram classification. This event occurred outside the core rainy season for this region, which typically occurs from 1 July to 15 September (Mathon et al., 2002). Its extreme character is more remarkable because of the amount of rainfall—131.5 mm (or 25.8% of the zonal mean total yearly precipitation amount)—recorded at the GARDAMA station. This extreme event (GARDAMA290404) was integrated into Group V_D (where the D index reflects a classification based on the dendrogram), which will be discussed later. This group includes all rainfall events generated by meteorological mechanisms covering different scales ranging from the local to synoptic and acting together.

The second extreme event (KOURESU060803) derived from the cut off of the first dendrogram node by (L_1) exceeded the cumulative thresholds for the sampling intervals from 30 min to 24 h, indicating the involvement of mesoscale to synoptic scale meteorological processes. Due to the significant quantity of rainfall (225 mm), which accounted for more than 40% of the recorded mean annual zonal total for 2003 over EPSAT, this case was isolated in group I_D. The other rain gauge stations where the 06 August 2003 rainfall event produced exceptional amounts of rain (HARIKAN and TANABER, see Table 3) exhibited quantities over the imposed threshold for the 5-year return period for duration ranges from 25 min to 24 h and 2–24 h, respectively. This clearly confirms that the 06 August 2003 rainfall event formed as a result of a combination of meteorological processes at the meso and synoptic scales.

A second imaginary vertical line ($\mathbf{L_2}$) was drawn to isolate 4 groups of extreme events. The first group (Group II_D) included an extreme event recorded on 02 June 2006 (TORODI020606). Revisiting the extreme events list (Table 3), we found that the TORODI event was characterized by rainfall above the fixed threshold for durations less than 1 h. This 30-min long event was classified as having derived from a localized system. The rain recorded at this station represented less than 15% (~11%) of the zonal mean annual total precipitation amount for the EPSAT area in 2006. The second group (Group III_D) was formed by 9 extreme events that arose from the following zonal rainfall events: 29 April 2004, which yielded extreme event signatures at 3 stations; 25 June 2008, which yielded extreme event signatures at 4 stations; and 6 August 2003 and 11 September 2008, both of which yielded extreme events at 1 station each. These events were characterized by rainfall with a return period greater than or equal to 5 years for interval durations typically between 30 min and 6 h, which correspond to temporal mesoscale characteristics. The most notable feature of this group was that the event rainfall amounts recorded in all cases exceed 20% of the annual zonal total precipitation amount for their respective occurrence years. In contrast, Group IV_D consisted of 3 extreme cases (TANABER060803, KOURE_SUD080709 and BOUBON140602), which were characterized by rainfall above the threshold for sampling intervals ranging from 2 h to 1 d (24 h), a trait associated with synoptic scale events. According to Janicot et al. (2008) and Reeds et al. (1977), African Easterly Waves (AEW) are the primary synoptic scale phenomena to occur during African monsoons and are associated with such lasting daily rainfall. Group IV_D may therefore result from these weather patterns. The extreme precipitation events in this group are characterized by rainfall between 15% and 20% of the zonal mean annual totals for the years they occurred. The fact that synoptic scale-derived rainfall events on 14 June 2002 (BOUBON140602) and 8 July 2009 (KOURE_SUD080709) yielded only one extreme localized rainfall case indicates that the occurrence of such extreme events in the EPSAT area do not depend on either the duration or the type of system present. Indeed, some mesoscale rainfall events in Group III_D (for example, the 25 June 2008 event that triggered 4 extreme data points) yielded much more extreme rainfall patterns than the synoptic-derived rain events on 14 June 2002 and 8 July 2009. As a result, we should consider these events' given weight in terms of rainfall proportion in the annual totals instead of their spatial and temporal extent. Finally, Group V_D was comprised of rainfall events that precipitated rain levels above the fixed threshold for almost all sampling intervals. This group consolidates the majority of extreme events observed over the EPSAT area for the study period (17 individual zonal rainfall events). These events were derived from the interaction between the different scale processes, ranging from the local to the synoptic, and were associated with 17 different zonal events. Events in this group are characterized by rainfall rates approximately 15 to 25% of the zonal mean annual total precipitation amount for their respective years. In total, of the 32 extreme events registered across the EPSAT area, 1 event (or 3.1%) was derived from a localized system (Group II_D), 9 (~28.1%) were derived from convective systems at the mesoscale (Group III_D), 1 event (3.1%) was derived from meteorological meso to synoptic scale disturbances (Group I_D), 3 (~9.4%) were the result of synoptic scale processes (Group IV_D) and 18 (~56.3%) were derived from interactions between the local, meso and synoptic scales (Group V_D).

The classification of these events using the proportion of

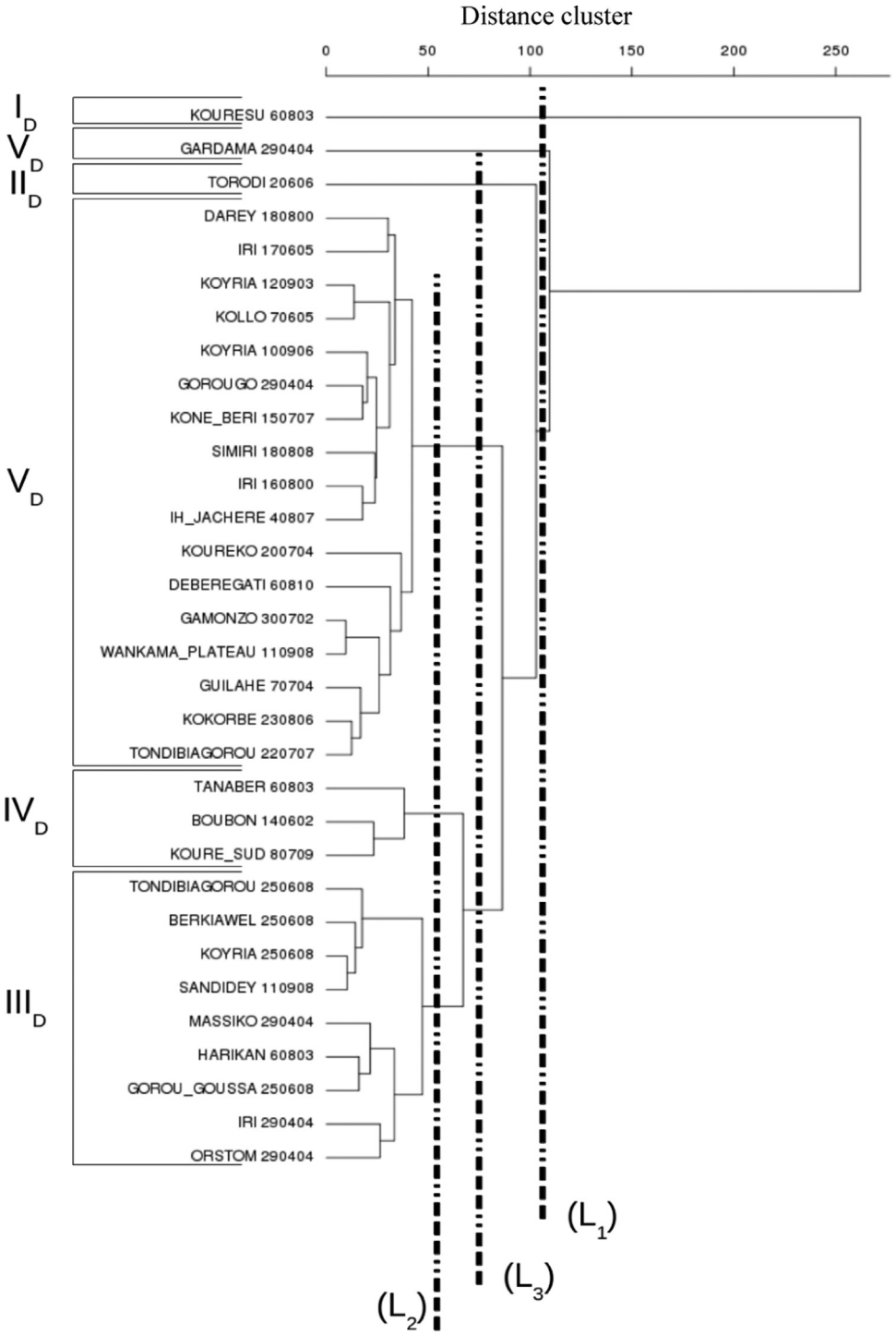

Fig. 9. Dendrogram of 32 extreme rainfall event cases on EPSAT area with return period equal or larger than 5 years for some of the studied durations (from 5 min to 24 h), obtained by the cluster analysis method. Dashed arbitrary vertical lines are used to determine groups. See the text for more details.

extreme rainfall instances related to the zonal annual totals generally transformed the EPSAT area groups derived from the dendrogram into three major homogeneous groups (as shown in Fig. 10). These are:

- Group I_R (where the index R classifies the group as a proportion of the extreme rainfall events), which is comprised of the TORODI020606 event (black point, Fig. 10b) derived from local scale phenomena (previously group II_D) and characterized by ratios less than 15%;
- Group II_R, which is comprised of the previously defined Groups III_D, IV_D, and V_D and which were derived by plotting the arbitrary vertical line L_2 on the dendrogram (Fig. 9). This group consolidates most of extreme event cases resulting from mesoscale, synoptic scale and combined local to synoptic scale meteorological disturbances. These events cases contribute between 15% and 25% of the zonal mean annual rainfall totals per year,
- Group III_R, which is comprised of the KOURESU060803 event (previously defined as Group I_D) and is marked by a rainfall amount equivalent to more than 25% (approximately 44%) of the zonal mean annual total precipitation in the year it occurred. On

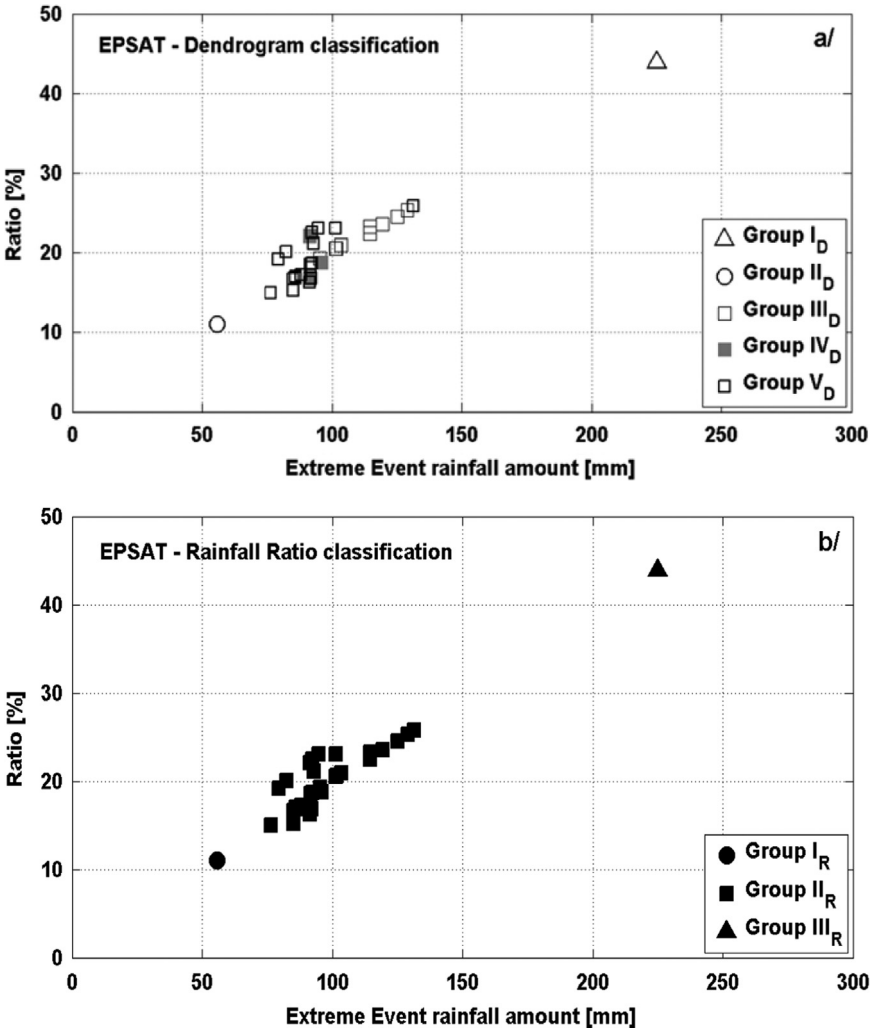

Fig. 10. Classification of EPSAT area 32 extreme event cases in the rainfall depth and proportion in the annual totals per year plan: (a) classification according to dendrogram method, (b) classification based on the ratio of rainfall events to annual totals per year. From panel (a) to (b), the symbols are held for groups finally merging according to ratio based classification.

the dendrogram (Fig. 9), this group was isolated by plotting the imaginary vertical line L_3, which indicated showing that this event occurred far from other events mapped in the dendrogram.

Classifying these events based on the proportion (weight) of extreme event precipitation related to the zonal mean total yearly precipitation reveals the homogeneity within extreme rainfall event groups. Groups I_R and III_R consist of extreme rainfall events that occurred outside the primary rainy season in the Sahel, which, according to Mathon et al. (2002), runs from 1 July to 15 September. Group II_R primarily consists of those extreme zonal rainfall events (21 of 22 zonal extreme rainfall events) that are essentially (75%) within the primary rainy season period in the Sahel. According to Mathon et al. (2002), who studied the same EPSAT area using combined satellite and rain gauge measurements, most of the zonal rainy events in the Sahel during this period (90%) are associated with organized convective systems (OCS), and the remainder are derived from a complex convective system called the MCC (Mesoscale Convective Complex). The fact that this group is composed of various meteorological scale events could be explained by the common mechanisms of merging or splitting of convective systems during an event's life cycle (Mathon and Laurent, 2001), which results in the integration of processes at different scales. Finally, the amount of rain produced by each extreme event in this group at a given station does not seem to be related to the event's duration because most events lasted 2 h and yielded different quantities of rain.

Similarly, when we plotted an arbitrary vertical line L_1 on the dendrogram for the OHHVO region (Fig. 11), we identified group I_D, which was comprised of two events (KOKO030910 and BIRNI230806) recorded on 3 September 2010 and 23 August 2006, respectively. In the Euclidian virtual space, these events were sufficiently far from other events, and the quantity of rain produced exceeded the threshold values for discrete time intervals from 10 min to 24 h. As a result, these events were identified has having been triggered by local to synoptic meteorological processes governing the formation of clouds and precipitation. The rainfall rates recorded at both stations were significant and accounted for 22.2% and 19.4% of the zonal mean annual totals for the years during which they occurred, respectively. For instance, 286.4 mm of rain were recorded in 6 h at the KOKO station in 2010, a year characterized by widespread inundations throughout Benin (Yabi and Afouda, 2012).

The division of nodes using L_2 allowed us to identify three additional extreme event groups, namely II_D, III_D and IV_D. Group II_D includes cases whose temporal characteristics indicate that they all originated from local scale clouds. Indeed, the maximum rainfall amounts recorded at a return period greater than or equal to 5 years occurred only for durations between 5 min and 30 min, which are characteristic of the local scale. In addition, for each of

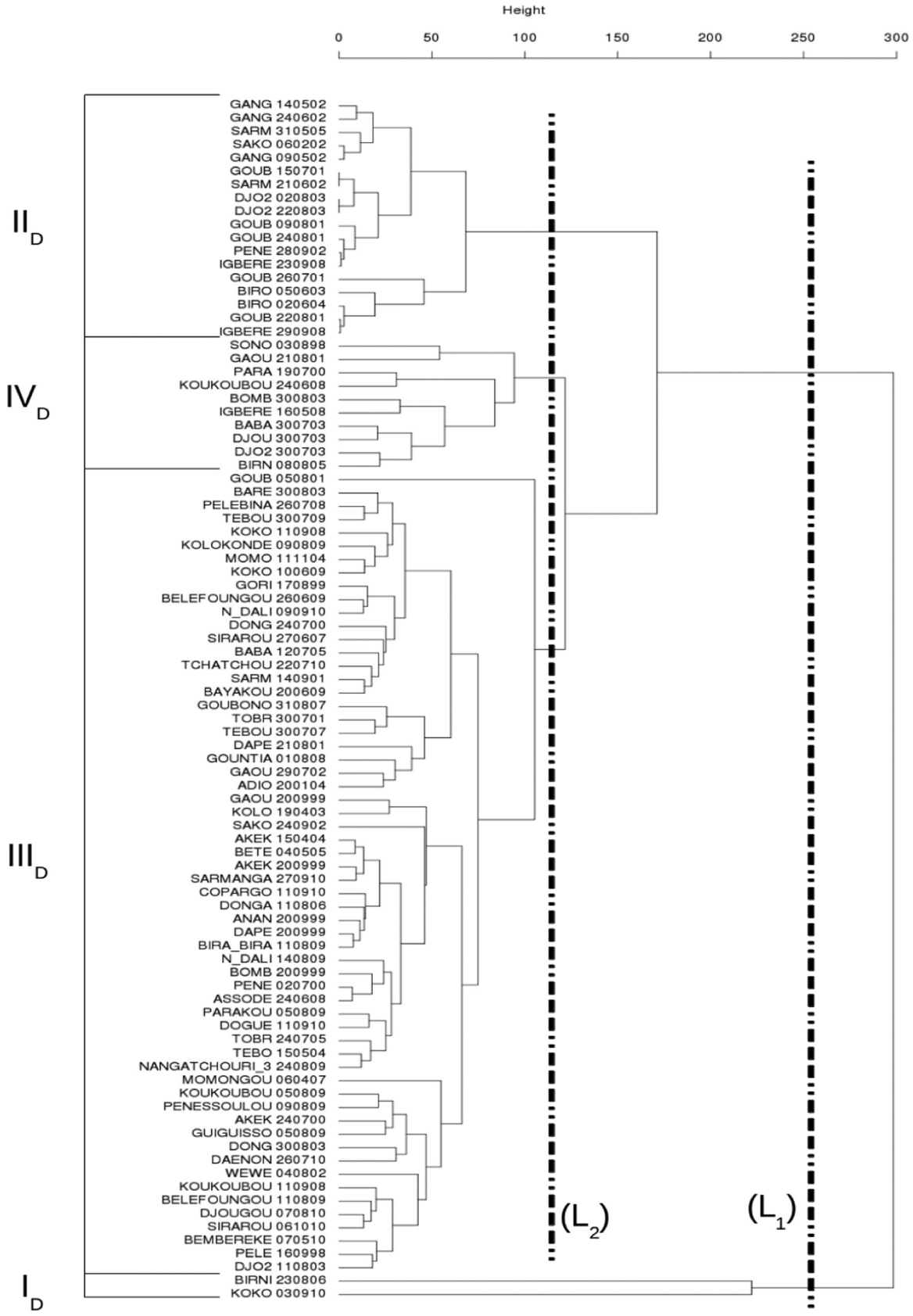

Fig. 11. Idem Fig. 9, but for the 90 extreme event cases on the soudanian OHHVO area.

the 18 events identified within this group, only one station experienced extreme rain, indicating the localized nature of the systems. This fact is confirmed by the durations of these event instances, which did not exceed 30 min. For all cases within this group, the proportions of extreme rainfall relative to the zonal annual totals for their respective years were below 6%. The second

group, III_D, derived from the plot of L_2 consisted of 60 extreme events instances (GOUB050801 to PELE160998, see Fig. 11) corresponding to 50 different zonal rainfall events. This group appears to be quite heterogeneous because the discrete time intervals for which rainfall maxima occurred at the 5-year recurrence level varied within different ranges (5 min to 2 h, 6–24 h, 30 min to 24 h, 2–24 h, 30 min to 12 h, 5 min to 6 h, 5 min to 24 h, to cite a few), suggesting that these events were affected by processes at all meteorological scales (local to synoptic). The ratio of event rainfall quantities to the annual totals lie in the range [6%; 15%]. The last group, IV_D, includes 10 extreme event instances characterized by rainfall over the threshold for the 5-year return period for sampling intervals ranging from 20 min to 24 h. These events may be derived from rain-related convective systems at the meso to synoptic scales. Rainfall levels recorded for these events at the stations where extreme instances occurred account for 10–25% of the zonal mean total yearly precipitation. According Casas et al. (2004), the main cause of rain-related floods is directly associated with extreme intense precipitation caused by large scale rainfall acting together with mesoscale convective systems. Hence, the highest ratios of extreme rainfall instances are consistent with the conclusions found in Casas et al. because most occurred in the primary rainfall season, during which AEWs (which govern synoptic patterns) coincide with mesoscale convective systems (Janicot et al., 2008). Nevertheless, a modelling approach would better illustrate how these processes result in such severe precipitation. One could also perform a multi-sensor analysis study (for example, study extreme event cases that occurred during the AMMA multi-sensor campaigns) to assess and forecast the processes that govern the formation of clouds anticipated to yield extremely intense rain. As an example of a future plausible investigation, we refer the reader to the work of Adachi et al. (2013), who designed a short-term forecasting method using volumetric C-band polarimetric radar to detect hazardous convective clouds. Their method outlined how to determine both the conditions and the onset time of localized intense rainfall from differential reflectivity radar data.

The classification of OHHVO extreme events according to their proportion of the zonal annual totals per year is notable. Fig. 12 illustrates that this parameter is a suitable criterion for distinguishing between extreme rainfall events in this area. Based on this criterion, the extreme precipitation events within the OHHVO area are classified into three major groups: (i) Group I_R, which consists of extreme rainfall instances with an annual precipitation ratio between 3% and 5% (black dots in Fig. 12b) (previously defined as Group II_D in the dendrogram); (ii) Group II_R, which includes events whose annual precipitation ratio ranges from 5% to 15% and are mainly related to Group III_D; and (iii) Group III_R, which merges Groups I_D and IV_D previously derived in the dendrogram.

Extreme events from the Group I_R in the OHHVO region unambiguously reflect the importance of local scale processes in their formation. However, events in Groups II_R and III_R are more complex and harder to define. To determine the nature of the convective precipitating systems in the OHHVO area, Depraetere et al. (2009) suggested event duration as a useful criterion. Because their work was based on rain gauge measurements,

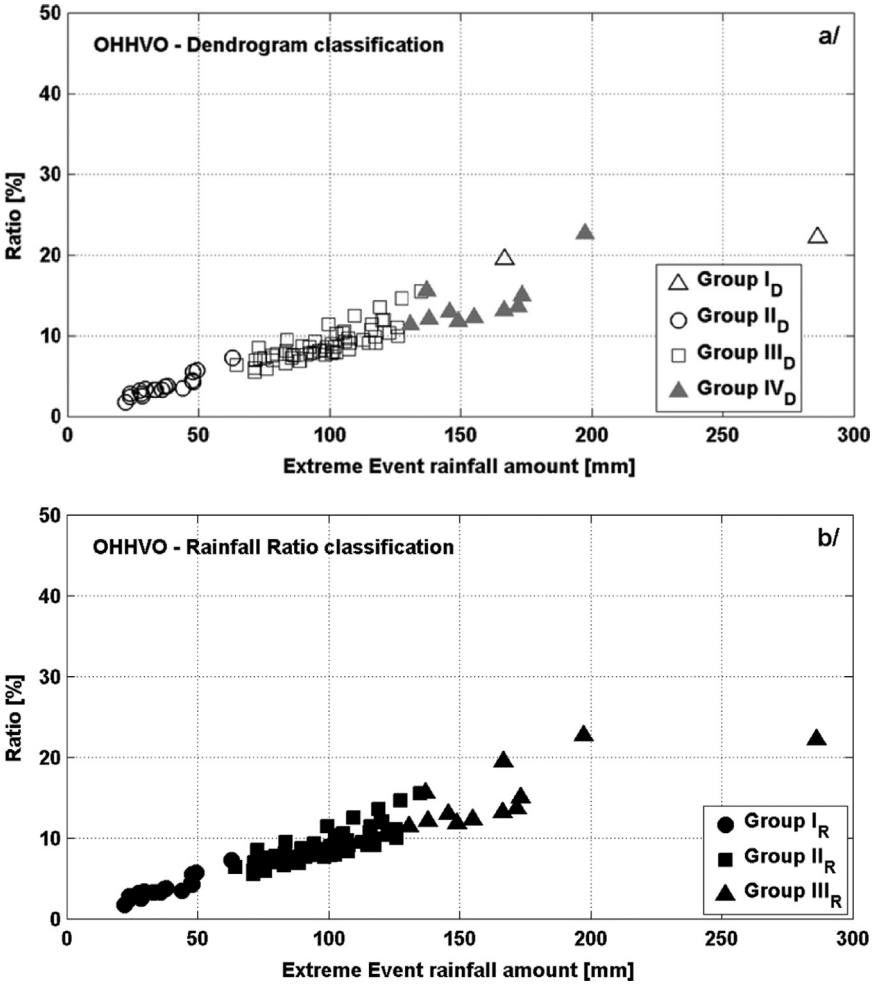

Fig. 12. Idem to Fig. 10, but for OHHVO zone extreme events cases.

including some from years also analysed in the present work (1999–2006), the present analysis of the potential origins of the events within these groups relies on event durations. The event duration intervals 1*h* (less than an hour),1 – 2*h*, 2 – 6*h* and 6*h* (more than 6 h) were used for this purpose. Fig. 13 shows the percentages of extreme events in Groups II_R and III_R according to their duration. This figure clearly reveals the heterogeneity of the extreme events within these primary groups. Group II_R is dominated by extreme events of mesoscale origin ("MCS-like" according to Depraetere et al. (2009)) including 35% that arose from mid-mesoscale (1–2 h duration) process and 50% derived from large mesoscale processes (2–6 h). The remaining events in this group (15%) were generated by local scale processes (10%) and synoptic scale meteorological disturbances 5%. Group III_R appears more heterogeneous than the II_R group. This group includes considerable discernible events that originated from mid-mesoscale (17%),

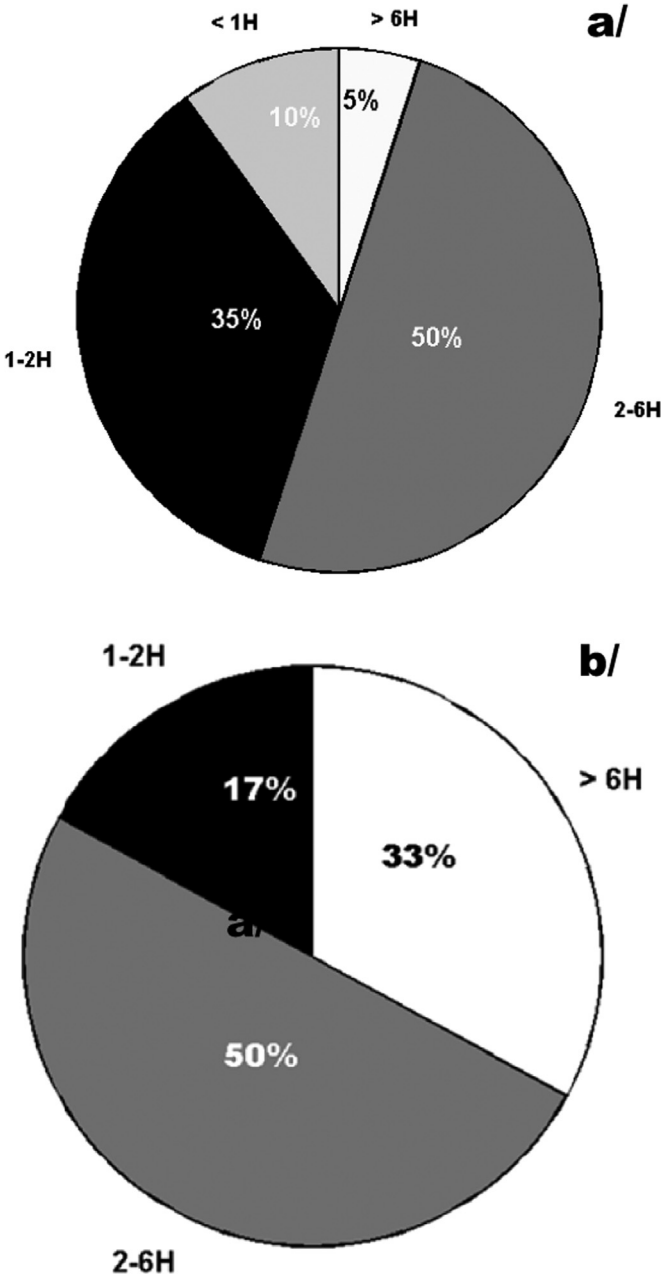

Fig. 13. Repartition of OHHVO Extreme events according their durations: (a) Major Group II_R, (b) Major Group III_R. See the text for further details about these major groups.

large mesoscale (50%), and synoptic scale (33%) meteorological processes. The events in the synoptic scale-derived subgroup have a mean duration of 12 h and are similar to convective systems classified by Depraetere et al. (2009) as "less organized type systems". This suggests that the interaction between different scale processes and the definition of problems need attention, especially if we are to provide a practical, meaningful way to interpret the nature of scale interactions leading to intense rainfall events.

Radar is a useful tool to illustrate the spatial organization of convective systems and evaluate the reliability of the rain gauge-based classification across the OHHVO study area. Indeed, the analysis of radar images provides an overview of the organized or disorganized character of various convective systems. During the intensive AMMA (African Monsoon Multidisciplinary Analysis) measuring campaigns in 2006 and 2007, an X-band polarimetric radar (Xport) system was used to sample northern Benin and characterize the spatial and temporal variability of rainfall on the ground, which had been insufficiently described by the additional OHHVO rain gauge network. Further details related to the configuration, operating parameters, and data processing techniques related to the radar data are provided in Gosset et al. (2010) and Koffi et al. (2014). Koffi et al. (2014) explored the AMMA radar dataset to show that the one-parameter polarimetric algorithm $R(K_{DP})$ performs well in retrieving rainfall rates above 30 mm/h relative to other estimators. In the present study, this algorithm is also used to derive rainfall fields from radar data. In Fig. 14, we show the spatial organization of two rainy systems included in Group II_R based on the radar reflectivity field identified at a time when these systems affected the stations recording extreme rainfall levels (Fig. 14a,c). This figure also shows the cumulative rainfall patterns mid- and one-third of the way through the life cycles of these two events, respectively (Fig. 14b,d). Both events were highlighted as extreme event instances via a rain gauge data analysis. One of these rainfall events, the 11 August 2006 case (Fig. 14a,b), which elicited extreme rainfall levels at the DONGA station (DONG110806), was accompanied by a squall line (convective organized system) structure. 50% of this event type occurred within 2–6 h. The second rainfall event (Fig. 14c,d), which occurred on 30 July 2007 lasted more than 6 h and was characterized by a less organized structure. Its spatiotemporal characteristics show that it was a stationary system that produced extreme rainfall at the TEBOU station (TEBO300707). This rainfall event was classified among the 5% of extreme events in Group II_R with a duration greater than 6 h.

4. Conclusions

Using data from two dense rain gauge networks at mesoscale sites located in the Sahel and Soudanian regions of West Africa, this study sampled rainfall events to analyse the extreme characteristics of rain across both areas. For each rainfall event, the maximum amount of rainfall for durations between 5 min and 24 h were sampled. We used the Gumbel extreme values distribution, IDF curves derived from observed maximum rainfall frequency distributions, and the theoretical IDF model outlined in Casas et al. (2004) to estimate the threshold for maximum rainfall rates; and we classified extreme rainfall instances according to their common characteristics.

Across the Sahelian zone, a total of 32 extreme rainfall events were counted, while 90 events were identified across the Soudanian zone. However, while it is known that it rains less in the Sahel than in the Soudanian area, we illustrated that the number of annual extreme rainfall events varied widely between the two regions. In particular, a dry region, such as the Sahel, was susceptible to much more frequent extreme events than the wetter OHHVO zone. These results confirm the spatial and temporal variability of precipitating systems in West Africa and show the

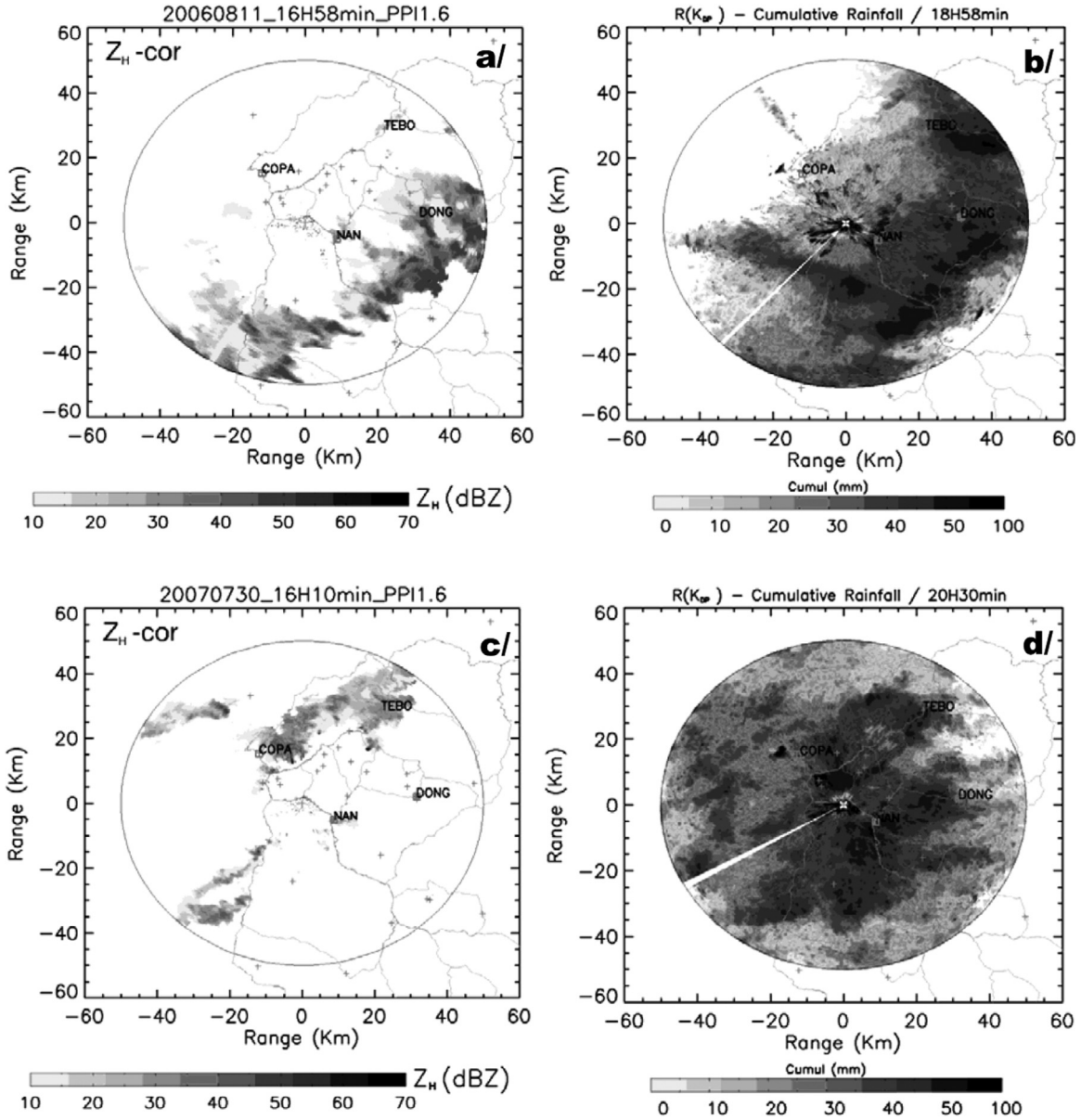

Fig. 14. Illustration of two rainfall event cases structure from the major group II_R that yielded exceptional rainfall intensities: (a, b) Rainfall event from a squall lines type convective system. DONGA station experienced extreme rainfall during this precipitation event (DONG110806), (c, d) Rainfall event from a less organized convective system. This MCS with duration more than 6 h affected TEBOU (TEBO300707) where it produced extreme rainfall. The left panels are the radar PPI corrected reflectivity when the systems reached the target station having recorded extreme values. In right hand panels are shown the corresponding mid- and one-third life duration total rainfall derived from $R(K_{DP})$ retrieval algorithm.

necessity of analysing extreme rainfall events based on the prevailing local, mesoscale and regional conditions in each climate zone. A cluster analysis based on the dendrogram revealed that other specific objective criteria for each region were needed to refine the classification of extreme rainfall events based on distinct meteorological processes at the various scales involved in extreme rainfall events. Thus, in the EPSAT Sahelian region, the mean contribution of extreme rainfall to total yearly precipitation values seems to accurately classify extreme events by providing information related to the severity of individual storms. It is clear from this classification that most of the extreme rainfall in the Sahelian area, with contributions ranging from 15% to 25%, is related to mesoscale convective systems occurring during the primary rainy season from 1 July – 15 September. This indicates that meteorological phenomena and the microphysical processes involved in the formation of these mesoscale precipitating systems are more homogeneous in this area. Nevertheless, certain events were characterized by mean contributions relative to total yearly precipitation (11% and ~44%) that differed from the homogeneous group of events mentioned above. These events occurred outside of the rainy season and during the onset of the rainy season.

In the Soudanian zone (OHHVO mesoscale site), the contribution criterion mentioned above allowed us to distinguish three major groups. One group clearly consisted of extreme events caused by local scale meteorological processes. However, the other two groups were characterized by the duration of the events. The heterogeneity of the latter two groups was significant in this area. These groups were comprised, in varying proportions depending on the given group, of events associated with local scale convection, mesoscale convective systems with durations lasting 1–6 h, and less organized mesoscale systems with durations greater than 6 h. Finally, the contributions of extreme precipitation events to total yearly precipitation values were a more important indicator in the Sahelian zone (10 to 45%) than in the Soudanian zone (2.5 to 25%), where

more than 95% of extreme events had a precipitation ratio below 16%. This southward decrease in the weight of the contribution of extreme events to total annual precipitation is consistent with Panthou et al.'s (2014) conclusions using the central Sahel extreme daily data analysis. For this reason, we classified extreme rainfall events according their severity within each zone.

The results obtained in the present study show the strong variability of intense rainfall at various spatial and temporal scales, leaving our results open for additional analysis. For instance, based on their classification, the possible cause-and-effect relationship between extreme rainfall events and their contribution to increasingly frequent flooding and urban inundations in the West African region should be further addressed and clarified. Such research would include an understanding of whether inundation is related to the unique extreme nature of precipitating systems or to other exogenous factors which must be taken into account. To this end, for specific sites with sparse rain gauge networks, one could revisit past rain gauge records and determine the contributions of rainfall events to mean total yearly precipitation to directly assess their extreme nature without relying on a dendrogram classification derived from a cluster analysis and identify their relationship to historic inundations.

Acknowledgments

Based on a French initiative, AMMA was built by year international scientific group and is currently funded by a large number of agencies, especially from France, UK, US and Africa. It has been the beneficiary of a major financial contribution from the European Community's Sixth Framework Research Program. Detailed information on scientific coordination and funding is available on the AMMA International web site http://www.amma-international.org. The authors thank the reviewers for their valuable contribution to improve the quality of this paper. The authors are indebted to the geophysical station of LAMTO (Côte d'Ivoire) for funding the publication fees of the article.

Appendix A. Supplementary material

Supplementary data associated with this article can be found in the online version at http://dx.doi.org/10.1016/j.wace.2016.05.001.

References

Adachi, A., Kobayashi, T., Yamauchi, H., Onogi, S., 2013. Detection of potentially hazardous convective clouds with a dual-polarized C-band radar. Atmos. Meas. Technol. 6, 2741–2760. http://dx.doi.org/10.5194/amt-6–2741–2013.

Alexander, L.V., Zhang, X., Peterson, T.C., Caesar, J., Gleason, B., Haylock, M., Collins, D., Trewin, B., Rahimzadeh, F., Tagipour, A., et al., 2006. Global observed changes in daily climate extreme temperature and precipitation. J. Geophys. Res. 111 (D05109).

Bouvier, C., 1986. Etude du ruissellement urbain à Niamey. Rapport général, Tome 3: Interprétation des données. Rapport CIEH-ORSTOM.

Casas, M.C., Codina, B., Redano, A., Lorente, J., 2004. A methodology to classify extreme rainfall events in the western Mediterranean area. Theor. Appl. Climatol. 77, 139–150. http://dx.doi.org/10.1007/s00704–003-0003-x.

Casas, M.C., Rodriguez, R., Redano, A., 2010. Analysis of extreme rainfall in Barcelona using a microscale rain gauge network. Meteorol. Appl. 17, 117–123. http://dx.doi.org/10.1002/met.166.

D'Amato, N., Lebel, T., 1998. On the characteristics of rainfall events in the Sahel with a view to the analysis of climatic variability. Int. J. Climatol. 18, 955–974.

Coles, S., 2001. An Introduction to Statistical Modelling of Extreme Values. Springer-Verlag, London.

Depraetere, C., Gosset, M., Ploix, S., Laurent, H., 2009. The organization and kinematics of tropical rainfall systems ground satelites tracked at mesoscale with assassins: first results from the campaigns 1999–2006 on the Upper Oueme Valley (Benin). J. Hydrol. 375, 143–160. http://dx.doi.org/10.1016/j.jhydrol.2009.01.011.

Di-Baldassarre, G., Montanari, A., Lins, H., Koutsoyiannis, D., Brandimarte, L., Blöschl, G., 2010. Flood fatalities in Africa: from diagnosis to mitigation. Geophys. Res. Lett. 37 (22), 1–5.

Djomou, Z.Y., Monkam, D., Lenouo, A., 2009. Spatial variability of rainfall regions in West Africa during the 20th century. Atmos. Sci. Lett. 10, 9–13.

Doswell, C.A., 1987. The distinction between large-scale and mesoscale contribution to severe convection: a case study example. Weather Forecast 2, 3–16.

Easterling, D.R., Evans, J.L., Groisman, P.Y., Karl, T.R., Kunkel, K.E., Ambenje, P., 2000. Observed variability and trends in extreme climate events: a brief review. Bull. Am. Meteorol. Soc. 81 (3), 417–426.

Estorge, J.L., Laborde, J.P., Zumstein, J.F., Mise en évidence des relations entre le gradex des pluies journalières et les gradex des pluies de durée inférieure à 24h en Lorraine. La Météorologie, Série VI, numéro spécial 20–21, Précipitations et Hydrologie, 1980, 1397–149.

Giorgi, F., Im, E.-S., Coppola, E.N., Diffenbaugh, S., Gao, X.J., Mariotti, L., Shi, Y., 2011. Higher hydroclimatic intensity with global warming. J. Clim. 24 (20), 5309–5324.

Goula, B.T.A., Soro, E.G., Kouassi, W., Srohourou, B., 2012. Trends and breaks at the level of daily rainfall extremes in the Ivory Coast (West Africa). Hydrol. Sci. J. 57 (6), 1067–1080.

Guhathakurta, P., Sreejith, O.P., Menon, P.A., 2011. Impact of climate change on extreme rainfall events and flood risk in India. J. Earth Syst. Sci. 120 (3), 359–373.

Janicot, S., Thorncroft, C.D., Ali, A., Asencio, N., Berry, G., Bock, O., Bourles, B., Caniaux, G., Chauvin, F., Deme, A., Kergoat, L., Lafore, J.-P., Lavaysse, C., Lebel, T., Marticorena, B., Mounier, F., Nedelec, P., Redelsperger, J.-L., Ravegnani, F., Reeves, C.E., Roca, R., de Rosnay, P, Schlager, H., Sultan, B., Tomasini, M., Ulanovsky, A., and ACMAD forecasters team. Large-scale overview of the summer monsoon over West Africa during the AMMA field experiment in 2006. Ann. Geophys. 26, 2008, 2569–2595.

Keggenhoff, I., Elizbarashvili, M., Amiri-Farahani, A., King, L., 2014. Trends in daily temperature and precipitation extremes over Georgia, 1971–2010. Weather Clim. Extrem. 4, 75–85.

Kieffer, A., Bois, P., 1997. Variabilités des caractéristiques statistiques des pluies extrêmes dans les Alpes françaises. Rev. Sci. Eau 2, 199–216.

Koffi, A.K., Gosset, M., Zahiri, E.-P., Ochou, A.D., Kacou, M., Cazenave, F., Assamoi, P., 2014. Evaluation of X-band polarimetric radar estimation of rainfall and rain drop size distribution parameters in West Africa. Atmos. Res. 143, 438–461.

Lebel, T., Parker, D.J., Flamant, C., Bourlès, B., Marticorena, B., Mougin, E., Peugeot, C., Diedhiou, A., Haywood, J.M., Ngamini, J.B., Polcher, J., Redelsperger, J.-L., Thorncroft, C.D., 2010. The AMMA field campaigns: Multiscale and multidisciplinary observations in the West African region. Q. J. R. Meteorol. Soc. 136 (s1), 8–33. http://dx.doi.org/10.1002/qj.486.

Lebel, T., Sauvageot, H., Desbois, M., Guillot, B., Hubert, P., 1992. Rainfall estimation in the Sahel: the EPSAT-Niger experiment. Hydrol. Sci. J. 37, 201–215.

Liebmann, B., Jones, C., Carvalho, L.M.V., 2001. Interannual variability of daily extreme precipitation events in the state of Sao Paulo, Brazil. J. Clim. 14, 208–218.

Mathon, V., Laurent, H., 2001. Life cycle of sahelian mesoscale convective cloud systems. Q. J. R. Meteorol. Soc. 127, 377–406.

Mathon, V., Laurent, H., Lebel, T., 2002. Mesoscale convective system rainfall in the Sahel. J. Appl. Meteor 41, 1081–1092.

Min, S.K., Zhang, X., Zwiers, F.W., Hegerl, G.C., 2011. Human contribution to more-intense precipitation extremes. Nature 470 (7334), 378–381.

Ndjendole, S., Perard, J., 2003. Estimation et spatialisation des durées de retour des fortes pluies en CentreAfrique. Publ. l'Association Int. Clim. 15, 319–325.

New, M., Hewitson, B., Stephenson, D.B., Tsiga, A., Kruger, A., Manhique, A., Gomez, B., Coelho, C.A.S., Masisi, D.N., Kululanga, E., et al., 2006. Evidence of trends in daily climate extremes over Southern and West Africa. J. Geophys. Res. 111, D14102.

Orlanski, I., 1975. A rational subdivision of scales for atmospheric processes. Bull. Am. Meteorol. Soc. 56, 527–530.

Pall, P., Allen, M.R., Stone, D.A., 2006. Testing the Clausius-Clapeyron constraint on changes in extreme precipitation under CO_2 warming. Clim. Dyn. 28 (4), 351–363.

Panthou, G., Vischel, T., Lebel, T., 2014. Recent trends in the regime of extreme rainfall in the central Sahel. Int. J. Climatol. 34, 3998–4006. http://dx.doi.org/10.1002/joc.3984.

Panthou, G., Vischel, T., Lebel, T., Blanchet, J., Quantin, G., Ali, A., 2012. Extreme rainfall in West Africa: a regional modeling. Water Resour. Res. 48, W08501. http://dx.doi.org/10.1029/2012WR012052.

Pilon, P.J., Adamowski, K., Alila, Y., 1991. Regional analysis of annual maxima precipitation using l-moments. Atmos. Res. 27, 81–92.

Reed, R.J., Norquist, D.C., Recker, E.E., 1977. The structure and properties of African wave disturbances as observed during Phase III of GATE. Mon. Weather Rev. 105, 17–33.

Smith, R.E., Schreiber, H.A., 1973. Point processes of seasonal thunderstorm rainfall distribution of rainfall events. Water Resour. Res. 10 (4), 871–884.

Thanoon, F.H., 2015. Robust regression by least absolute deviations method. Int. J. Stat. Appl. 5 (3), 109–112. http://dx.doi.org/10.5923/j.statistics.20150503.02.

Thunis, P., Bornstein, R., 1996. Hierarchy of mesoscale flow assumptions and equations. J. Atmos. Sci. 53, 380–397.

Yabi, I., Afouda, F., 2012. Extreme rainfall years in Benin (West Africa). Quat. Int. 262, 39–43. http://dx.doi.org/10.1016/j.quaint.2010.12.010.

Zhang, Q., Chen, X., Becker, S., 2011. Spatio-temporal variations of precipitation extremes in the Yangtze River Basin (1960–2002). China. *Atmos. Clim. Sci.* 1, 1–8. http://dx.doi.org/10.4236/acs.2011.11001.